STRUCTURAL AND SPECTRAL STUDIES OF SUNSPOTS

Grant NGR 39-005-066

NATIONAL AERONAUTICS AND SPACE ADMINISTRATION

Final Report

Period: September 1, 1967 - August 31, 1974

Principal Investigator: Arne A. Wyller

Bartol Research Foundation
of
The Franklin Institute
Swarthmore, Pennsylvania
19081

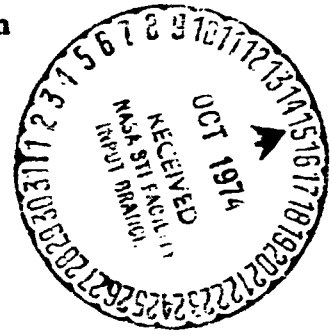

Submitted: October 9, 1974

TABLE OF CONTENTS

I. Summary

At the Bartol Coudé Observatory we have continued our observations of umbral cores, both by multicolor photometry and by narrow-band photometry in the vicinity of the sodium D lines. These observations have indicated that no single umbral model can account for all of the observed umbral cores. To speak of "the" model of an umbra is therefore not meaningful. In a series of observations of one spot at a variety of positions on the disk, it has been found that the sunspot exhibits limb brightening. Furthermore, the weakening of sodium absorption near the limb (relative to that at disk center) is much more pronounced than any model currently predicts. Both these results imply that the upper atmosphere of this spot is hotter than any current model predicts, and may in fact have a temperature inversion at the level where the D lines are formed. Of the models currently available we believe that Kneer's (1972) model comes closest to agreeing with the observations, although even that model cannot explain all of the available observations.

Theoretical work on Alfvén wave propagation in the atmosphere of a spot has been followed numerically to first order in the wave amplitude. In regions where the wavelength exceeds the density scale height, the wave flux is found to decrease with

altitude in accordance with the WKB solution. But in the upper photosphere and chromosphere, where the density scale height is small compared with the wavelength, the first order solution indicates a flux diverging at great height. Attempts to incorporate second-order terms in the wave amplitude are continuing.

Our observations of excess flux around sunspots suggest that a significant fraction of the missing flux in sunspots may appear as a slight brightening in a large area surrounding spots. A time-dependent model of turbulent heat transfer indicates that turbulent diffusion by supergranules can account for the observed excesses in some cases. Sound waves also can transport energy laterally away from spots.

The Alfvén-wave model developed for sunspots has been extended to the case of starspots on flare stars and on the primary component of contact binaries. The model has been successful in accounting for a wide variety of observations in these objects, and this gives us further confidence that the models developed for sunspots are indeed realistic. Effects of magnetic fields on solar neutrinos are shown to be negligible.

II. Observational Work with the Bartol Coudé Telescope

a. Narrow Band Observations of Umbral Cores

Observations of the intensity of sunspots have been continued on those clear days when suitably large spots were present on the disk. Solar activity has unfortunately declined during the past year, and we have observed only about a dozen spots this year, mostly of small umbral area.

The observations which we have concentrated on are an investigation of the maximum intensity between the sodium D-lines. In figure 1, we show an idealized portion of the spectrum of a spot in the vicinity of the D-lines. We measure intensity, both in the umbral core and at the center of the solar disk at three wavelengths, 5874.125 Å, 5893.4 Å, and 5931.75 Å, using wavelength resolution of 0.2 Å. The first and third wavelengths are at the center of continuum windows in the umbral spectrum, as listed by Wöhl (1970). Interpolation in wavelength between these two windows allows a determination of the continuum intensity I_A at 5893.4 Å, which is the wavelength where the umbral spectrum has maximum intensity between the D-lines according to the Göttingen umbral atlas. I_A is obtained both in the spot and at the solar center. The direct measurements of the intensity at 5893.4 Å yields I_B again both in the spot and at the center of the disk. In

the disk spectrum, where the D-lines are narrow enough that the wings do not overlap appreciably, I_B (sun) = I_A (sun). We therefore obtain

$$r_{spot} = \frac{I_B\ (spot)}{I_A\ (spot)} = \frac{I_B\ (spot)}{I_B\ (sun)} \Big/ \frac{I_A\ (spot)}{I_A\ (sun)}$$

We use this, in combination with the intensity ratio

$$R_{spot} = \frac{I_A\ (spot)}{I_A\ (sun)}$$

to define a two-dimensional classification system for umbral spectra. As with all umbral measurements, both r and R must be corrected for scattered light. We have assumed, as before, that by sitting in the umbral core, where the spot intensity consistently falls to the same low level, we have essentially thereby isolated the intensity of the umbral core, unaffected by blurring, and affected only by large angle scattering. The latter has been found to be a remarkably constant function for our instrument. The procedure of correcting for scattered light is therefore simply to measure the aureole intensity at a distance of one arc minute off the limb of the sun, and multiply this by a factor Z. The value of Z becomes larger the closer the spot is to the disk center, and can be as large as 7-8. In presenting the results for spots near the disk center (Figure 2) we have indicated a range of values adopted for Z typically, Z = 4 to Z = 8. Near the limb, we choose

Z = 1-3 typically. The advantage of our two-dimensional classification system for umbral spectra is then immediately apparent, since scattered light corrections enter in a correlated fashion in the two dimensions. Hence instead of uncertainties due to scattered light making their appearance as error boxes, in this diagram, the uncertainties appear as lines. The length of a line in the Figure is an indication of the scattered light in the instrument. On and before July 7, 1973, the scattered light was almost 1% at one arc minute from the limb, causing the lines of July 7 and February 28, 1973 to be very long. On and after August 30, 1973, following a cleaning of the siderostat and 8-inch diaphragm, the scattered light fell to 0.4-0.5%, and this is reflected in the shorter lines for the later observations.

Theoretically, each sunspot model yields just one point in this diagram, at least for spots at disk center, $\mu = 1$. The values of μ for different spots is indicated in the figure. Five models are shown, due to Kneer (1972), Stellmacher and Wiehr (1972), Yun (1971), and two revised models of Yun's (reported in the annual report for the period September 72 - September 73, Section III.A), denoted YI and YII in the figure. All theoretical points move upwards and to the right as a spot moves towards the limb (but not enough to explain the results in Figure 2, see below).

Of special interest in Figure 2 is the series of observations for a spot from July 9 to July 17, 1974, during which time the spot longitude varied from 64° East to 40° West. The intensity of the continuum decreased near the center of the disk, indicating limb brightening from about 10% at disk center to 13% at 64° longitude. Note that all our intensities are quoted relative to the intensity of the center of the solar disk. If we were to give intensities relative to the solar intensity at equal distance from the disk center, the limb brightening would become even more pronounced. Thus $I^*(\theta=0)/I^\odot(\theta=0) = 0.10$, and $I^*(\theta=64^\circ)/I^\odot(\theta=64^\circ) = 0.20$. The good agreement between observations on July 11 and July 17 when the spot was equidistant from the central meridian is an indication that the spot structure remained essentially unchanged in this six-day period. This spot therefore seems to be a good candidate for testing limb-darkening predictions. Since the observations at disk center (July 12) coincide well with Kneer's model, it is encouraging to see that Kneer's model predicts limb brightening, although not as much as 30% from $\mu=1$ to $\mu=0.6_4$, (cf. Fig. 4 of Zwaan (1974) which is drawn for $\lambda=5000$ Å). The model of Yun (1971) also predicts limb brightening at 5890 Å, by a factor of 30%, although the continuum is too bright to be in agreement with present observations. On the contrary, the models of Stellmacher-Wiehr (1972) and of Zwaan (1974) predict limb darkening. The conclusion is that

for the umbral core in the spot which crossed the solar disk in 1974, July 9-17, the model which best fits the observations is probably that of Kneer.

Apart from the limb brightening in the continuum, the most obvious feature of Figure 2 is the fact that the line absorption is very much reduced near the limb. This is obvious not only from the observations on one spot in July but in all spots with $\mu=\cos\theta=0.6$ or less. In all such cases, the line absorption is so weak that r_{spot} rises to 0.9, compared with 0.5 - 0.7 near disk center. This is a sensitive test of umbral models, because it depends on two widely separated levels of the umbral atmosphere ($\tau \approx 0.1$ - 0.01 and τ = 1-2). Stellmacher and Wiehr (1972) have computed the center-to-limb variation of r_{spot} for 4 models (cf. their figure 2). From $\mu=1$ to $\mu=0.5$, the value of r_{spot} increases from 0.46-0.55, 0.22-0.28, 0.58-0.73, and 0.77 to 0.80. Clearly none of these four models is adequate to explain the much larger dependence of r_{spot} on μ which we have observed. All of the models give lines which are too deep near the limb, indicating that the temperatures in the upper layers of all these models are too low. This conclusion is of course strengthened by the observations of limb brightening in the spot of July 1974. In fact these latter observations require the presence of a temperature inversion, the amplitude of which cannot, however,

be estimated without extensive computer modelling of the radiative transfer. In view of the sparseness of the currently available data, we believe that to embark on an extensive series of trial and error radiative solutions at this time would not be fruitful. Zwaan (1968) points out the inevitability of a temperature inversion due to lateral influx of radiation. The inversion, he expects, should set in at $\tau \simeq 0.01$ in large spots, and perhaps as deep as $\tau \approx 0.1$ in small umbrae. He presented some tentative evidence based on molecular lines to prove the existence of the inversion, although a synthetic spectrum analysis of the MgH molecular bands using the temperature-inverted model has been shown by Branch (1970) to lead to disagreement with observations. Here we believe that we have obtained for the first time some evidence (at this time qualitative) based on atomic lines for the existence of the inversion in the atmospheric layers where the sodium lines are formed.

This however does not change our conclusion that no single model fits all of the spot observations, and so every spot appears to be different, even in the deeper layers where the continuum is formed.

In the continuum at 5893.4 A, the intensities of the umbral cores (R_{spot}) extend over a wide range even near the

center of the disk, R_{spot} = 6.5 - 24%. The lower limit which we have observed coincides well with the darkest spot observed by Ekmann and Maltby (1974) at λ = 5790 A (I = 6.5 $\pm$ 1.0%) while the upper limit which we have observed is much higher than other observers have indicated (cf. Figure 1 of Zwaan, 1974).

It is apparent that (i) no two spots have the same physical characteristics in both the atmospheric region where the wings of the sodium D lines are formed and in the region where the continuum is formed; (ii) none of the theoretical model points lies on any of the observed lines, suggesting that none of these models gives a satisfactory explanation of both line-forming and continuum - forming layers of a spot. In fact, the observations indicate that it is hardly meaningful to talk of "the" model of a sunspot umbra. Every umbra appears to be unique, at least within the range of umbral sizes included in the diagram, A_u = 8 to 60 millionths of a solar hemisphere. It is therefore difficult for us to agree with the suggestion of Rossbach and Schröter (1969) that umbrae of all sizes have essentially identical physical conditions. Although this might be the case in the deeper layers of the umbra (Henoux, 1969), there must arise differences in the upper layers, close to and above $\tau \approx 1$, where on the one hand photospheric radiation begins to illuminate the dark gas in the umbra, and on the other hand the magnetic field geometry

is modifying itself in order to adjust to hydrostatic equilibrium with the much lower gas pressures in the upper layers. Thus the assumption of a simple uniform field is acceptable at great depths, where it is permissible to write

$$p_{spot} + B^2/8\pi = p_{sun} \qquad (1)$$

(p = gas pressure, B = field strength). However, equation (1) is certainly not applicable within 200-300 km of the photosphere, where the pressure of a spot field of 2-3 kilogauss actually exceeds p_{sun}, so that the above relation becomes meaningless. The field geometry presumably changes to a force-free configuration by the time it reaches the chromosphere, and this change presumably begins at depths of 200-300 km below the photosphere, where curvature terms must be added to the left-hand side of equation (1). Since each spot finds itself in a different active region, each spot must adjust its deep field to different boundary conditions in the force-free region. Thus it is expected that the variation of magnetic field with depth is different for each spot, so that each spot has its own pressure variation, and accompanying $T = T(\tau)$. The variations from spot to spot in Figure 2 may therefore be correlated either with the strength and geometry of magnetic fields in the active regions surrounding each spot, or with the diameter of the umbra, and its effect on lateral radiative

influx. In the absence of detailed magnetographic coverage of each active region, we cannot at the moment test this hypothesis, but the need for magnetographic information in the vicinity of spots will also become apparent in discussing the excess flux around spots (see below).

b. Broad-Band Observations of Umbral Cores

Two spots were observed in broad band. One of these, observed on two days in July 1974, gave results as shown in Figure 3. The observations were corrected for scattered light by applying a correction factor Z = 6 to the observed aureole intensity at one arc-minute from the limb. In Figure 3, the observations are compared with the five theoretical models referred to in Figure 2. On the basis of these broad-band observations, it appears that none of the five models is really suitable for this spot. From the results in Figure 3, it is difficult to avoid the conclusion that there are great differences in intensity from one spot to another. The large spot (A_u = 80) observed on October 30, 1972, and plotted also in Figure 3 is clearly darker, by a factor of at least two, than the small spot (A_u = 35).

The efficacy of broad-band observations of spots is clearly minimal in view of corrections due to differential line blanketing which must be applied to the observations.

Our observations suggest that the variation of intensity of umbral cores with wavelength is not even monotonic. If this is due to errors in the differential blanketing corrections, then clearly broad-band observations of spots cannot be used to set constraints on umbral models.

c. Magnetometer

On July 17, 1974, a spot at μ=0.76 was investigated with the magnetometer. The observations were noisy, and they showed circular polarization rising to +3.6% at $\Delta\lambda$ = 0.26 Å from the center of the D_2 line. However, the sign of polarization did not change going through the center of the line, but remained positive at $\Delta\lambda$ both positive and negative. This may indicate that the field lines of the spot (viewed at an angle of 40° to the local vertical) were more or less transverse to the line of sight so that the signal detected was actually a component of elliptical polarization.

d. Search for the Missing Flux of Sunspots.

Following a suggestion of R.E. Danielson, we have undertaken an observational program which is aimed at searching the vicinity of sunspots for the possible presence of missing flux. It is possible that the flux which is missing from a spot is redistributed over a wide area surrounding the spot, so that the intensity of the photosphere would be increased above

normal in the vicinity of the spot. Up to the present time, this excess of flux has never been detected around spots, partly because of limits of sensitivity of photographic techniques. In the worst cases, photographs might fail to detect excesses smaller than about 4% of the normal disk intensity (Bray and Loughhead, 1964), so that even if the missing flux were confined within an area of only 25 times the umbral area (assuming for simplicity that the umbra is perfectly dark, and no flux is missing from the penumbra), the excess flux would have been missed. Since the penumbral area is typically 4-5 times the umbral area, the excess flux would have to be confined to an area centered on the umbra with a diameter of no more than 2.2 - 2.5 times the penumbral diameter, in order to be detected. (The "bright-ring" observed by Waldmeier (see Bray and Loughhead, 1964) is a different effect, closely confined to the penumbral-photosphere boundary, and in all probability simply due to overshooting penumbral bright filaments (Danielson, 1973)).

The fact that no observations have yet detected an excess flux around spots suggests that if this is indeed the correct explanation of the missing flux, then the excess must be spread out over a much larger area of the solar surface, producing thereby an excess too small to be detected by photographic sensitivity. (However, very recently, Miller (1974) has

succeeded in detecting the excess photographically in some cases. See below.)

The sensitivity of the Bartol coudé telescope is, however, essentially limited only by the electronics which prevent photon counting rates from exceeding 10^7 counts/second. Thus sensitivity of 0.1% is easily achieved, and if systematic effects can be excluded, the Bartol instrument is capable of detecting the excess flux if it were to be spread over an area with diameter as large as 15 times the penumbral diameter.

We have searched for the flux surrounding spots on October 26, 1973, (A_u = 15), November 15, 1973 (A_u = 4), and January 13, 1974 (A_u = 35). On the latter two days, sky conditions were not good enough over a long period to obtain spectral observations of the spots concerned. In particular, on January 13, there were intermittent clouds, so that the results are hardly meaningful. The spot on November 15 was very small, so we will confine our remarks here to the results of October 26. The spot concerned was large, A = 370, but there was more than one umbra, the largest having as umbral area of only A_u = 15. The spot's position was 17°E 15°S (μ = 0.955). The telescope was stepped in declination starting at the center of the largest umbra, in steps of 2" per second, and the photon counts were recorded. Results are in Figure 4,

where each dot indicates the counts in one second of time, starting in the umbra at radial distance r = 0. The scan continues to a radial distance of about 5 times the penumbral radius, so the equivalent area is 25 times the penumbral area or 550 times the area of the largest umbra.

The statistical uncertainty in the counting rates is indicated, and is obviously much smaller than the observed variations from second to second. The latter are probably due to real fluctuations in brightness in the photosphere, since our entrance aperture, 1."6 corresponds very closely to the mean diameter of granules (1100 km) on the solar disk. Granular contrast is known to be as large as $\pm$ 5% (Bahng and Schwarzschild, 1961), and this would certainly suffice to explain the variations.

More significant, however, is the gradual decrease in the counts with increasing distance from the spot. It is necessary first to remove limb darkening effects, for the scan extends along 10% of the solar diameter. The limb darkening has been calculated approximately along the scanning path, and is shown in Figure 4. It actually slopes upward towards the right, and so the gradual decrease of intensity away from the spot is enhanced. The dashed line through the points has an area in excess of the normal solar flux (represented by the curve labelled "limb darkening") which is sufficient to compen-

sate for the area missing in the spot, i.e. the area enclosed by the dash-dot line within the penumbra.

Because the jog mode of guiding the telescope is most relia le in the north-south direction, we restricted our scans t. that direction. Thus, we have only a one-dimensional scan of what must surely be a two-dimensional feature. Nevertheless, it appears that we may indeed have succeeded in detecting the missi g flux around this spot, making its appearance in the form of an excess of flux spread over a wide area surrounding the spot. We return to a theoretical discussion of the effect below.

An interesting confirmation of our results has been provided by Miller (1974), who used photographic means to detect excess brightness around spots. The excess brightness observed by Miller may sometimes be as high as 7% of the normal disk intensity, and he believes that this excess may account for as much as 50% (if not more) of the missing flux.

III. Theoretical Studies at the Bartol Observatory

a. Theoretical Zeeman Profiles of the Sodium D_2 Line

While Dr. Hong Sik Yun was at Bartol, he had partially completed a computer program aimed at integrating numerically the equations of transfer in the Stokes parameters I, Q, and V.

This program has now been completed, and debugged so that now the Zeeman profile can be computed for an arbitrary line in an arbitrary model atmosphere. In particular, the sunspot model of Kneer (1972) has been used to fit a theoretical profile to the observations of the D_2 line in a spot on August 30, 1973. (The observations were reported in last year's annual report.) The resulting curve fits the observed points somewhat better than the points are fitted by theoretical results computed using Yun's spot model, but the error bars on the observations are so large that there is little reason to prefer one model over the other on the basis of these observations.

It has now become clear why Yun's initial estimates of expected circular polarization in the wings of the D lines were so small. He used Unno's (1956) theory for the Zeeman effect, which requires a knowledge of the ratio of line to continuum absorption coefficients η at each point in the line profile. The procedure is to evaluate this ratio at the line center, where $\eta = \eta_o$, by fitting the observed line depth at line center with a theoretical line profile in the absence of any magnetic field. Then η can be evaluated at each point in the line profile by assuming that the line absorption coefficient has a Doppler profile, appropriately shifted in each polarization by the Zeeman splitting. However, in the program written by Yun, η was evaluated independently at each

point in the profile, and in particular was evaluated with physical conditions pertaining to one particular optical depth in the atmosphere, $\tau = 0.001$. Since the effective level of line formation varies across the line, in the sense that in the far wings, the line is formed deeper than $\tau = 0.001$, and in the core the line is formed at shallower layers than $\tau = 0.001$, the result is that the polarization is overestimated in the wings and underestimated in the core of the line.

The program for numerical integration of the equations of transfer in polarized light has been modified to include more exact boundary conditions at the lower boundary of the atmosphere. Rather than simply setting I = B (where B is the Planck function), and Q = V = 0 there, we now use the more exact conditions suggested by Beckers (1969). However, the line profiles do not appear to be significantly affected by this change.

A significant check on the numerical integrations is that the intensity I at the top of the atmosphere should approximate closely that evaluated by an eight-point formula for the intensity integral given by Zwaan (1965). If the numerical integration has been terminated at an optical depth which is too large, then the numerically integrated line will not appear as deep as that predicted by Zwaan's formula. We have found that at a distance of 0.6 Å from line center, integration up to $\tau = 0.001$

ensures accuracy within 0.6%. At larger distances from line center, it is not necessary to carry the integration upwards as far into the upper atmosphere, while closer to the line center, in order to achieve accuracies of better than 1%, it is necessary to integrate higher up than $\tau = 0.001$.

b. Zeeman Profiles of Other Lines

In a preliminary attempt to extend the program to Zeeman profiles observed in magnetic stars, we have considered the profile of the line due to neutral chromium at 4254 Å, a line which in the past has been observed in spots while URSIES was located at the Flower and Cook Observatory in Paoli. This line is particularly interesting because it is the line which was used by Borra et al (1973) to search for weak magnetic fields in stars, using a Zeeman polarimeter essentially identical to the one we use at Bartol for sunspots. Borra et al give a line profile observed in the magnetic star β Coronae Borealis. We have computed Zeeman intensities of the Cr I line using three model atmospheres for this star. The models were provided (by private communications) by S. Adelman, J. Hardorp, and R. Friedman, with effective temperatures of respectively 10^4, 8750, and 8600°K. The peak in the observed polarization at $\Delta\lambda = 0.12$ Å is reproduced, with a degree of polarization of 24%. However, these numerical integrations of intensity are only the first step in computing stellar

profiles, for these require further integration over the surface of the star. Such an integration would be extremely time-consuming, and hardly justifiable in view of our lack of detailed information about the distribution of magnetic fields, limb darkening, and microturbulent velocities over the surface of the star.

c. Turbulent Heat Conduction and the Missing Flux in Sunspots

Again following a suggestion of R.E. Danielson, we have investigated the horizontal transfer of heat away from a spot by turbulent convection. We idealize the spot as a cylinder of radius a($\simeq 10^4$ km) from which energy is to be transported across the curved surface. The heat flux emerging from the cylindrical walls of the spot is assumed to be equal to the missing flux integrated over the total spot area, Q($\approx 10^{29}$ ergs/sec). The coefficient of thermal diffusivity outside the spot is set equal to $\alpha = 0.1\ C_s \lambda x$, where C_s is the local sound speed, and $\lambda = ax$ is the "mean free path" of the turbulent conducting elements, expressed as a fraction x of the spot radius. The problem then is the following: given a region bounded on the inside by a cylinder of radius a, across which heat flows outward at a rate Q, what value must x ($=\lambda/a$) have in order that the heat distribution outside the cylinder is compatible with our observations of the excess flux in the neighborhood of sunspots?

To answer this, we need the solution to the cylindrical heat transfer problem, as tabulated numerically by Ingersoll et al (1950). Outside a cylinder transferring heat at a constant rate of q ergs per second per unit length of cylinder, the excess temperatures at radial distance r at time t is given by

$$\Delta T = \frac{q}{k} G(z,p)$$

where $p = r/a$, k = thermal conductivity, $z = \alpha t/a^2$, $\alpha = k/\rho C_p$ is the thermal diffusivity, ρ = gas density, C_p = specific heat at constant pressure. The function $G(z,p)$ is an integral over zero and first order Bessel functions and Neumann's Bessel functions of the second kind. G is tabulated for four radial distances by Ingersoll et al, $p = 1,2,5,10$. (Note: $p = 1$ is the outside boundary of the cylinder). The tabulated values are shown in Figure 5.

For the purposes of computation, a model of the solar convection zone due to Baker and Temesvary (1966) was used. This gives values of C_s, ρ, C_p, and temperature as a function of depth below the top of the convection zone, i.e. as a function of depth below the undisturbed photosphere, essentially (since convection in the sun sets in close to optical depth $\tau = 2/3$; cf. Mullan, 1971). A value must be assumed for the depth of the spot, since ΔT above is expressed in heat flow q per unit length. We have pointed out reasons for taking the depth of a

spot equal to 10^4 km (Mullan, 1972; 1973a) so this is what we assume here. The missing flux is taken to be

$$Q = \pi a^2 F_s \ (A_u(1-I_u) + A_p(1-I_p))$$

where $F_s = 6.33 \times 10^{10}$ ergs/cm^2/sec is the solar flux; A_u, A_p are the fractions of the total spot area occupied by umbra and penumbra respectively; and I_u, I_p are the intensities of umbra and penumbra in units of the disk intensity. With $a = 10^9$ cm, $A_u = 0.25$, $I_u = 0.1$, $I_p = 0.7$, we have $Q = 8.95 \times 10^{28}$ ergs/sec.

The problem is time dependent, so the bright ring around a spot diffuses outwards with time, and becomes weaker in intensity at any given point. The weakest the intensity can be occurs when the spot is as old as possible. Let us take a time $t = 0.1\ A_{max}$, which is the mean lifetime, in days, of a spot or spot group having a maximum area of A_{max} millionths of a solar hemisphere, (Bray and Loughhead, 1964). Then we can ask: what is the excess flux expected at the outer edge of the penumbra ($p = 1$) for a spot of area $A_{max} = 100$ at age $t = 10$ days, given that x may vary over a range of values? We have set $x = 0.003$, 0.06, 0.03, 0.1 and 0.3 and calculated excess temperatures ΔT as a function of depth. ΔT is a rapidly decreasing function of depth, so that we need only consider the top-most 1. :rs of the sun. As an extreme case, let us consider the level of the Wilson depression, which is about

1000 km below the photosphere (Yun, 1970). At this depth, the excess temperatures are found to be the following:

TABLE 1

x	0.003	0.01	0.03	0.1	0.3
$\Delta T(^{\circ}K)$	4342	2082	1004	425	184
$\Delta F/F(\%)$	114	55	26	10	5

The excess flux at the edge of the penumbra, ΔF, is computed in terms of the normal solar flux approximately by $\Delta F/F = 4\Delta T/T$ where T is the undisturbed temperature in the sun at a depth of 1000 km, $T = 15242^{\circ}K$. It is apparent that unless $x > 0.3$, the excess flux even at this late time in the history of the spot, would have been easily detected even by photographic photometry. Is it possible to have $x > 0.3$? Presumably what is doing the turbulent convection around a spot is the convection zone, with diffusivity having such a value that supergranules can survive the erosion of turbulent conditions for only about 20 hours. With length scales of $(2\text{-}4) \times 10^4$ km, such lifetimes correspond to diffusivities of $\alpha = (0.6\text{-}2.2) \times 10^{14}$ cm^2/sec. At $z = 10^3$ km depth, $C_s = 12$ km/sec, and hence such α's correspond to $x = 0.5\text{-}2$. Thus it appears that it might be marginally possible to explain the excess fluxes at the very end of spot lifetimes by this method. However, at earlier phases of a spot's life, say after one or two days, $\Delta F/F$ is expected to

exceed 5% even if x is as large as 0.5-2, simply because the excess heat is crowded into a smaller area surrounding the spot. Further investigations are called for before a definite answer can be given, but, these preliminary results suggest that turbulent heat conduction away from spots is not really capable of explaining the missing flux in spots.

d. Sound Waves and the Missing Flux in Sunspots

Danielson and Savage (1968) suggested that the missing flux might be carried away from the spot by horizontally propagating magnetosonic waves. Outside the spot, these become sound waves, and it is important to test the hypothesis of whether the missing flux might be sound waves, rather than turbulent convection as in the preceding sub-section.

The important quantity is the dissipation length for sound waves travelling through the undisturbed solar gas outside a spot. Formulae for absorption of sound in a medium of very high thermal conductivity (such as the sun, where radiation ensures high conductivity even if turbulence were totally absent) are given by Landau and Lifshitz (1959). The result simplifies in the limit of wave frequency much greater or much less than the characteristic frequency $\omega_c = C_s^2/\alpha$. With $\alpha = 0.1 C_s ax$, we have $\omega_c = 10 C_s/ax$. At depths of 1-10 thousand km below the surface, C_s = 12-30 km/sec, and so with $a = 10^9$ cm, $\omega_c = (0.012\text{-}0.03)/x$. Danielson and Savage (1968) note that

wave periods at great depth in the sunspot are expected to be about 1/2 hour, i.e. $\omega = 0.0035$. Hence with $x \sim 1$ (see previous sub-section), $\omega << \omega_c$, and the absorption length is

$$\lambda_{abs} = \frac{2c_s^3}{\omega^2 a(\gamma-1)} = \frac{20c_s^2}{\omega^2 ax(\gamma-1)}$$

where γ is the ratio of specific heats. Setting $\gamma \leq 5/3$, $x = 1$, $a = 10^9$ cm, $c_s = 20$ km/sec, $\omega = 0.0035$/sec, we find $\lambda_{abs} \gtrsim 10^{10}$ cm. It therefore appears that low frequency sound waves could propagate away from the spot over several spot radii before dissipation. Hence sound wave propagation away from spots is a mechanism which is worth considering as a possible explanation of the missing flux in spots.

e. Chromospheric Heating Above Spots by Alfven Waves

The problem of chromospheric heating above sunspots involves not the horizontally propagating waves, as in the previous subsection, but vertically propagating waves. Since the field lines in the deeper layers of a spot are close to vertical, it is natural to consider the waves in question as Alfvén waves. Such waves have the advantage of very long dissipation lengths in spots (Osterbrock, 1961), so that once they are produced, these waves can essentially propagate undissipated all the way to the surface layers of the spot. Thus the flux of Alfvén waves, once they are generated, should

remain constant with height. This can be proven analytically, using the WKB approximation (Alfvén and Fälthammar, 1963) which shows that in a medium where the density and magnetic field varies only very slowly over one wavelength of an Alfvén wave, the amplitude of the wave, b, is independent of the field strength and varies as $b \sim \rho^{1/4}$ (Cowling, 1953). Then the energy flux in the waves, $F_A \sim b^2 V_A$, where V_A is the Alfvén speed, is independent of density, and $F_A \sim B$, the mean field strength. In a spot model, such as that used for the sunspot models (Mullan, 1974) where B is taken to be independent of height, F_A is constant. The conditions for the WKB approximation to be valid are satisfied to a certain extent throughout the depth of the spot, but are especially well satisfied near the top of the spot where most of the Alfvén wave flux is generated (see Figure 7 of Mullan, 1974). Thus the wavelength of the waves, (see Figure 3 of Mullan, 1974) is essentially one pressure scale height, H_p, and so the condition for the WKB solution to be valid is that $H_p \ll H_\rho$, where H_ρ is the density scale height. It is easy to show that

$$\frac{H_p}{H_\rho} = 1 - (1-Q)\nabla$$

where $\nabla = d\,\ell n T / d\,\ell n P$ is a dimensionless temperature gradient, and $Q = d\,\ell n\,\mu / d\,\ell n T$ is a dimensionless gradient of molecular weight. Due to ionization effects, $Q < 0$, so an upper limit

on H_p/H_ρ is $1-\nabla$. In deep layers where ionization is almost complete $\nabla = 0.4$, and H_ρ exceeds H_p by a factor of almost 2. In layers near the surface, where ionization is in progress $|Q|$ increases and ∇ approaches unity (or even exceeds it in some models). Then H_ρ becomes much greater than H_p, and WKB conditions are well satisfied.

So far, our models have dealt only with conditions below the Wilson depression, i.e. at depths > 1000 km, where the field can reasonably be expected to be uniform. Now we must consider the propagation of the Alfvén waves emerging from the "surface of the spot" (i.e. the Wilson depression) as these waves enter atmospheric layers where (i) the field is no longer uniform, and (ii) the density varies so rapidly with height that the WKB approximation no longer holds.

As regards (ii), Pikelner and Livshits (1965) claim that the flux of Alfvén waves should vary as $F_A \sim \rho^{1/2}$. They derive this result from formulae which are applicable to reflection and transmission of Alfvén waves from a discontinuity in density (cf, e.g. Alfvén and Fälthammar, 1963). Thus Pikelner and Livshits argue that the variation of density in the visible layers of a spot is so rapid (H_ρ < wavelength) that it is permissible to consider the gas density as varying discontinuously from the photosphere into the chromosphere-corona. Formulae have been derived for this case if the field remains perpendicular

to the boundary and of constant strength across the discontinuity. Then the flux transmitted is

$$T = \frac{F_{Trans}}{F_{incident}} = \frac{4\sqrt{\rho_1\rho_2}}{(\sqrt{\rho_1} + \sqrt{\rho_2})^2}$$

where ρ_1, ρ_2 are the densities on either side of the discontinuity. In Figure 6, the ratio T is plotted as a function of ρ_1/ρ_2. It is seen to decrease slowly at first ($\rho_1/\rho_2 \approx 1$), in accordance with the WKB solution that if the density varies infinitely slowly, the flux is constant, and all of the incident flux must be transmitted, so that T = 1. The larger ρ_1/ρ_2 becomes, the farther the curve departs from the WKB solution (T = 1). However, it is clear that to write $F_A \sim \rho^{1/2}$, as Pikelner and Livshits have done, is too drastic, and results in transmission of too little flux to the less dense medium. In the limit $\rho_1/\rho_2 >> 1$, Pikelner and Livshits underestimate the transmitted flux by a factor of 4; and in the opposite limit, $\rho_1/\rho_2 \approx 1$, their solution does not approach smoothly to the WKB limit.

As a specific example, we may consider the case of an Alfvén wave generated at the bottom of the convection zone, where $\rho_1 = 3.1 \times 10^{-6}$ g/cm^3. By the time this wave reaches the "top" of the spot (i.e. the Wilson depression, see Mullan, 1974), where $\rho_2 = 4.6 \times 10^{-7}$ g/cm^3, it has traversed gas where $\rho_1/\rho_2 = 6.7$. In Figure 6 this point is indicated on all curves. The assumption

in our model of sunspots is that T = 1, which is probably a valid solution since WKB conditions are well satisfied. In the opposite extreme, if the density variation from bottom to top of the spot were encountered by the Alfvén wave as a discontinuity, then 20% of the waves would be reflected, and T = 0.8. At most, then, not more than 20% of the upcoming flux should be lost, whereas according to Pikelner and Livshits, more than 60% of the upcoming flux should be reflected. Thus their estimate of reflected flux is three times larger than that predicted even in the extreme case of replacing the density gradient by a discontinuity. Since in fact most Alfvén waves in the spot models are generated near the "top" of the spot, ρ_1/ρ_2 is even smaller than 6.7, and the T curve approaches even more closely to the WKB solution, so that Pikelner and Livshits' estimate of reflected flux becomes even more incorrect near the top of the spot.

A more serious criticism of Pikelner and Livshits' approach, however, is that they claim that they are considering energy <u>flux</u>, whereas in fact they have introduced the area of a flux tube (in order to avoid considering field variations) so that their result actually applies to <u>luminosity</u> (ergs/sec) rather than flux (ergs/cm^2/sec). When their formulae are rewritten in terms of flux, it is found that the flux must include the field strength, which certainly varies in the upper layers of a spot. However, the formula for T above was derived in the case of constant B, and

is therefore not applicable to the present case. It is therefore not permissible to consider chromospheric heating by Alfvén waves, and by fast and slow magnetosonic waves, according to the method described by Pikelner and Livshits, and later developed numerically by Marik (1967).

It is certainly to be expected that it is permissible to replace a continuously variable medium by a discontinuity in order to study wave reflection, if the wavelength is short compared with the density scale height. Justification for this expectation is provided, at least in the gas-dynamic case, by the work of Chisnell (1955) who showed that when a shock impinges on a region where the density varies smoothly from ρ_1 to ρ_2, the strength of both reflected and transmitted waves agrees well with the results obtained if the shock impinges on a discontinuity where the density rises abruptly from ρ_1 to ρ_2. A shock is however a more extreme case than we are considering here, and the principal problem associated with Alfvén wave propagation in a spot is this: the wavelength of the wave, λ, is initially (at great depths) small compared with the local density scale height, $\lambda \ll H_\rho$, but in propagating upwards the Alfvén speed grows, and the density scale height falls, until eventually near the photosphere ($Z \approx 0$, on the scale where the Wilson depression is $Z \approx -1000$ km) λ becomes larger than H_ρ. In the topmost layers of the upper photosphere and low chromo-

sphere, assuming that the wave frequency remains equal to that at excitation (period $\approx 10^2$ - 10^3 seconds), λ eventually becomes extremely large compared with H_ρ. It appears that only a numerical solution can cope with conditions where λ/H_ρ assumes values which are both less than unity and greater than unity.

The theoretical picture becomes more complicated if the field is not perpendicular to the discontinuity. All three hydromagnetic wave modes are coupled together, especially if the incident waves move nearly parallel to the field lines (Stein, 1971). The solid angle centered on the field lines within which coupling of modes is strong is proportional to $(\Delta\rho/\rho)^2$ where $\Delta\rho$ is the discontinuity in density at the boundary. In the limit of continuous variation of density, the coupling goes to zero unless the direction of the magnetic field rotates with altitude. In the latter case Alfvén waves propagating through a stratified medium couple with the fast-mode waves (Frisch, 1964).

The propagation of hydromagnetic waves in a stratified medium in absence of mode-coupling (i.e. in the absence of field rotation) was discussed by Ferraro (1954), and later by Ferraro and Plumpton (1958). They assumed a uniform field, and applied the boundary condition that the wave amplitude must go to zero at large altitudes. The solution depends on the ratio of λ to H_ρ. When $\lambda \ll H_\rho$, the amplitude of velocity in the wave varies as predicted by the WKB approx-

imation $v \propto \rho^{-1/4}$, at high densities. Eventually, however, the decreasing density causes λ to exceed H_ρ, and then the velocity amplitude decays rapidly to zero, $v \propto \rho^{1/2}$. Thus even in a uniform field, the flux of energy would decay proportional to $\rho^{3/2}$ in the upper atmosphere. The wave distorts as it propagates upwards, in the sense that gravity inhibits vertical motions and causes the wave to become polarized horizontally.

Hollweg (1972) criticized the boundary condition used by Ferraro and Plumpton, and proposed that a more correct boundary condition is to require that there are no waves coming in from infinity. Hollweg retained the case of constant vertical field, but extended their analysis to a stratified medium with two scale heights, one small at low altitudes, the other large at great altitudes. This is a good approximation to the solar chromosphere. The solution found by Hollweg behaves as expected in the WKB limit, namely $v \propto \rho^{-1/4}$. However, in the non-WKB limit, $\lambda/H_\rho >> 1$, the amplitude continues to increase with height, although more slowly than in the WKB case: $v \propto \log (\lambda/H_\rho)$. The normal hydromagnetic relation between velocity amplitude v and magnetic amplitude b does not hold in the non-WKB case, and b becomes constant in the upper atmosphere.

It is a feature of non-WKB propagation that reflection can occur even if the density is continuous. A discontinuity in scale height serves to reflect a non-WKB wave. The flux

leaking upwards into the chromosphere depends on how much is reflected at the discontinuity in scale height. For the special case considered by Hollweg, only about 1/6 of the upward moving flux can leak through to the chromosphere. We have extended Hollweg's results to the general case of the discontinuity in scale height occurring at an arbitrary altitude. The transmission coefficient T can be obtained in the limit of wavelength much larger than scale height by using the asymptotic expansions of the J_0 and Y_0 Bessel functions:

$$T = \frac{4\beta\gamma}{(\beta+\gamma)^2 + \frac{4}{\pi^2}(\gamma \ell n\gamma - \beta \ell n\beta)^2}$$

where $\beta = 2Z_{01}\omega/V_{02}$ and $\gamma = \beta Z_{02}/Z_{01}$. Here, ω is the wave frequency, Z_{01} is the scale height near the photosphere, $Z_{02}(>Z_{01})$ is the scale height in the chromosphere, and V_{02} is the Alfvén speed at the altitude where the scale height is discontinuous. If the discontinuity in scale height is shifted up in the chromosphere to a density 100 times smaller than that considered by Hollweg, we find T = 0.05, which is smaller than the value obtained by Hollweg by a factor of only 3 or 4. Thus the leakage of non-WKB waves into the chromosphere is not sensitive to the density at which the chromospheric temperature rise sets in. The altitude of the temperature minimum can alter by several hundred kilometers without essentially changing the transmission coefficient, at least in the case of constant

magnetic field.

In an attempt to extend Hollweg's analysis to the case of a non-uniform field, we consider Hollweg's equation for the wave amplitude ν as a function of the modified height variable $\zeta = e^{-Z/2Z_0}$:

$$\nu'' + \zeta^{-1}\nu' + \alpha^2 \nu = 0 \qquad \text{(H-2)}$$

where prime denotes differentation with respect to ζ, and $\alpha^2 = 4Z_0^2\omega^2/V_0^2$. In Hollweg's case, V_0 is the Alfvén speed at height $Z = 0$, and is therefore proportional to B_0, the assumed constant field. The case of varying field can be represented by allowing α^2 to vary with altitude. Since B is expected to decrease at great heights, α^2 must increase as Z increases i.e. α^2 must increase as ζ decreases. Suppose we write then

$$\alpha^2 = \alpha_0^2 + (\mu^2/\zeta^2)$$

where α_0 is the value of α deep in the photosphere. Then equation (H-2) becomes

$$\nu'' + \nu' y^{-1} + (1+\mu^2/y^2)\nu = 0$$

where $y = \alpha_0\zeta$ and primes denote differentiation with respect to y. The above equation has a solution which can be considered as a Bessel function of imaginary order. The solution is given by Boole (1844):

$$\nu = \cos(\mu \ell n y)\left[1 + a_2 y^2 + a_4 y^4 + \ldots\right]$$

where coefficients a_2, a_4 etc. reduce to those appropriate for the zeroth order Bessel function $J_0(v)$ in the limit $\mu = 0$. There is a corresponding series solution, singular at $y = 0$, corresponding

to $Y_0(y)$. The numerical values of α_0 can be obtained approximately by setting $\zeta = 1$, $Z_0 = 185$ km, $\omega = 0.02$ sec^{-1}, $V_0 = 10^6$ cm sec^{-1} (appropriate for a sunspot with B = 3000 gauss, $\rho = 7 \times 10^{-7}$ gm cm^{-3}). Then $\alpha_0 = 0.74$. At the top of the atmosphere, say Z = 2000 km, where B has decreased to 300 gauss, α^2 must have increased by a factor of 100, so that $\mu^2 = 99\ \alpha_0^2 \exp(-2000/185)$, or $\mu \approx 10^{-4}$. Then the modification of the J_0 solution for ν due to non-zero μ is the factor $\cos\left(10^4 \left[\ln\ \alpha_0 - (Z/Z_0)\right]\right)$. As long as we are interested only in wave propagation within a few tens of scale heights distance from Z = 0, this factor cannot depart from unity by more than a few parts in 10^6. This suggests that as long as the field varies with altitude in a way which is much slower than the variation of density, then the full solution of the wave equation should approximate the (J_0, Y_0) solution obtained by Hollweg. However, the best test for this is to obtain a numerical solution.

We have attempted to derive a numerical solution as follows. The usual hydromagnetic equations are written in the form (Deift and Goertz, 1973):

$$\frac{\partial \underline{B}}{\partial t} = \nabla \times (\underline{\nu} \times \underline{B}) \qquad (1)$$

$$\nabla \cdot \underline{B} = 0$$

$$\rho \left[\frac{\partial \underline{\nu}}{\partial t} + \underline{\nu} \cdot \nabla \underline{\nu}\right] = -\nabla \left[\frac{B^2}{8\pi} + p + \psi\right] + \frac{\underline{B} \cdot \nabla \underline{B}}{4\pi} \qquad (2)$$

$$\nabla \cdot (\rho \nu) = 0$$

where ψ is the potential including (if necessary) gravitational and centrifugal terms. The field of the spot is written in cylindrical coordinates as $B_0 = (B_r, 0, B_z)$. The field of the Alfvén wave, and its associated velocity amplitude, are written as $(b_r, 0, b_z)$ and $(\nu_r, 0, \nu_z)$ respectively. In the absence of waves, $\nabla \cdot \underline{B}_0 = 0$, and so to satisfy $\nabla \cdot \underline{B} = 0$ in the presence of the waves, we have $\nabla \cdot \underline{b} = 0$. It is assumed that in the absence of waves, the field satisfies

$$\nabla \left(\frac{B_0^2}{8\pi} + p + \psi\right) = \frac{\underline{B}_0 \cdot \nabla \underline{B}_0}{4\pi}$$

This is the assumption of magnetohydrostatic equilibrium, including curvature forces, and it presupposes that the spot is a stable entity. It is assumed that in the perturbed state we may keep terms of first order only. Then since variations of pressure in an Alfvén wave are of second order (Alfvén and Fälthammar, 1963) we neglect δp. Also, in an Alfvén wave $\underline{B}_0 \cdot \underline{b} = 0$, and so to first order B^2 remains unchanged. Assuming that variations in ψ are also of second order, the perturbed version of equation (2) is

$$\rho \frac{\partial \underline{\nu}}{\partial t} = \left(\frac{\underline{B} \cdot \nabla \underline{B}}{4\pi} \right)_{\text{first order terms}}$$

combining this with the perturbed version of equation (1), and noting that $b_r/b_z = -B_z/B_r$ in a wave where b_θ is assumed to remain identically zero, we obtain the following equation for b_r:

$$\frac{\partial^2 b_r}{\partial z^2} + \frac{\partial b_r}{\partial z}\left[\frac{1}{H_\rho} + \frac{\partial}{\partial z}(\ell n U) + \frac{V}{U}\right] + b_r\left[\frac{V}{UH_\rho} + \frac{1}{U}\frac{\partial V}{\partial z} + \frac{4\pi\omega^2\rho}{U}\right] = 0 \quad (3)$$

where the wave has been assumed to be sinusoidal with frequency ω, and the quantities U and V are the following:

$$U = B^4/B_z^2$$

$$V = -\frac{B^2}{r}\frac{B_r}{B_z} + \frac{B^2}{B_z}\left\{\frac{\partial b_r}{\partial r} + \frac{B_r}{B_z}\frac{\partial B_r}{\partial z} - \frac{B_r}{B_z}\frac{\partial B_z}{\partial r} - \frac{B_r^2}{B_z^2}\frac{\partial B_z}{\partial z}\right\}$$

and $B^2 = B_r^2 + B_z^2$.

As background field, we have taken that suggested by Yun (1970):

$$B_z(r,z) = D(\alpha)\,\zeta^2$$

$$B_r(r,z) = -\alpha D(\alpha)\frac{d\zeta}{dz}$$

$$D(\alpha) = (\Phi/\pi)\exp(-\alpha^2)$$

$$\alpha = r\zeta(z)$$

$$\zeta(z) = (\pi B_z(0,z)/\Phi)^{1/2}$$

Φ = magnetic flux through the spot.

Once the vertical field along the axis is specified, $B_z(0,z)$, these equations define the magnetic field at all r and z. Along the axis we have taken $B_z(0,0) = 3000$ gauss, and a gradient of -1 gauss/km so that the spot field is no longer vertical at altitudes of 3000 km above the center of the spot.

To solve for the amplitude b_r, two boundary conditions are necessary. At the moment, the two we have chosen are the following: (i) $b_r(0,0) = 10^3$ gauss; this ensures that the local flux of Alfvén waves at the center of the spot at $z = 0$ is approximately equal to that generated in our sunspot model with $B = 3000$ gauss (Mullan, 1974); the numerical value of b_r, though, is simply a scaling factor as far as the solution is concerned; (ii) assume the umbra is uniformly dark, then the flux of Alfvén waves must be constant at all radii at $z = 0$ (in this integration, $z = 0$ is located at the level of the Wilson depression, at which we presume we know the flux of Alfvén waves entering from below); thus

$$b^2 B = \text{constant} = b_r^2(0,0) B_z(0,0) = 3 \times 10^9$$

This leads to

$$b_r(r,0) = \frac{b_r(0,0) \exp(\alpha^2/2)}{\left[1 + (B_r^2/B_z^2)\right]^{3/4}}$$

Hence $\partial b_r/\partial r$ is known at $z = 0$, and $\nabla \cdot \underline{b} = 0$ then leads to an expression for $\partial b_r/\partial z$ at all radii in the umbra at $z = 0$. At each radial position in the umbra, then, equation (3) can be integrated upwards numerically, once the variation of density with height has been specified. We assume (see Mullan, 1974) that the density in the spot is equal to the density in the undisturbed sun, so that the density could ideally be read off

from, say, the BCA model (Gingerich and de Jager, 1968). However, numerical differentiation of this model leads to a non-monotonic variation of density scale height (cf. Jordan, 1970), and since it is preferable to keep all functions varying as smoothly as possible, we have decided to choose H_ρ initially to have a smooth variation with height, following as closely as possible the BCA variation for those regions of the atmosphere where BCA is relevant. In the deeper layers, near Z = 0, we have used interpolated H_ρ values between the deepest BCA value and the value in our sunspot model at the Wilson depression. Then choosing the density to be equal to BCA density at the level of minimum H_ρ ($\rho = 1.43 \times 10^{-8}$ gm/cm^3 at H_ρ = 107 km), we derive the model as in the table:

TABLE 2

Z(km)	ρ(gm/cm^3)	H_ρ(km)
0	8.79×10^{-7}	1900
150	7.93×10^{-7}	1190
300	6.83×10^{-7}	832
450	5.53×10^{-7}	584
600	4.09×10^{-7}	409
750	2.65×10^{-7}	286
900	1.43×10^{-7}	200
1050	5.52×10^{-8}	115
1200	1.43×10^{-8}	107
1350	3.54×10^{-9}	108
1500	8.89×10^{-10}	109
1650	2.27×10^{-10}	111
1800	5.96×10^{-11}	113
1950	1.61×10^{-11}	116
2100	4.51×10^{-12}	120
2250	1.33×10^{-12}	125
2400	4.12×10^{-13}	132
2550	1.40×10^{-13}	145
2700	5.39×10^{-14}	170
2850	2.39×10^{-14}	200

The height scale is such that z = 796 corresponds to "Height = 0" in the BCA model. The density in the table follows the density in the BCA model in the chromosphere very well, departing from it by no more than 25% even at the topmost heights. The deeper layers do not agree as well with the run of density derived in our sunspot models. Thus at z = 0, the density in Table 2 exceeds that in our sunspot model at the Wilson depression by 85%. However, this is not excessive, and the solution using Table 2 should preserve the major features of the solution using a more detailed variation of density with height.

The period chosen for the waves is 300 seconds. This is the period of waves excited at the Wilson depression, in our spot model if we set the period equal to the local cell height (H_p) divided by the convective velocity (v_c). It takes gas a period of time of this order to circulate around a cell and thereby generate an Alfvén wave according to the scheme of Figure 3 of Mullan (1974). In a spot with B = 3000 gauss, we find $H_p \approx 220$ km, $v_c \approx 0.75$ km/sec. Therefore, $H_p/v_c = 294$ seconds. In spots with B = 2000 and 4000 gauss, we find H_p/v = 240 and 350 seconds respectively. A period of 300 sec is long enough that internal gravity wave excitation in the atmosphere is expected to reflect some of the Alfvén waves back down into the spot. Most of the waves should be transmitted, however, since I = 70% (Danielson and Savage, 1968, especially Figure

in their paper). We therefore expect the wave flux upwards to be reduced by about 30%. At first, the numerical solution for the flux on the axis of the spot does indeed show a decrease with height, dropping off to 65% of incident at a height of 600 km above z = 0, i.e. at a depth of about 240 km below the undisturbed photosphere. Above z = 500 km, however, the flux begins to increase with height (see Figure 7).

Away from the axis of the spot, where the field direction is not vertical, the vertical flux is smaller than on axis (at z = 0). The flux at these positions, however, also shows an increase of flux with height (see Figure 7).

These flux increases are not physically acceptable, but it is not yet clear what is causing the increases. Numerical errors may be involved, or perhaps second order terms need to be retained in the perturbation equations. Another possibility is that we have encountered a resonance peak of the type discussed by Hollweg (1972, especially his Figure 2). The principal peak occurs when $\alpha_0 = 2Z_{01}\omega/V_{01}$ equals the first zero of the Bessel function J_0. In our case, with $\omega = 0.02$, $V_{01} = 10$ km/sec, we find $J_0(\alpha) = 0$ if $Z_{01} \approx 500$ km. At such a peak, the flux may rise to ten times (or more) the WKB flux. Another possibility is that mode-mode coupling becomes important when the wavelength of the wave ($\lambda = 220$ km = pressure scale height at the Wilson depression) approaches, and becomes less than, H_ρ.

According to Table 2 above, this should occur at z = 800 km.

For any reasonable wave period, the Alfvén wavelength λ inevitably exceeds the density scale height H_ρ in the upper atmosphere, although the wavelength is less than the density scale height deep below the surface at (say) the level of the Wilson depression. In an attempt to make the transition from $\lambda<H_\rho$ to $\lambda>H_\rho$ smoother, we have computed model atmospheres for umbrae using the computational method of Mihalas (1967). We have assumed that temperatures in the umbra differ from those in the Harvard-Smithsonian Reference Atmosphere (HSRA) by $\Delta\theta$ = constant (where $\theta = 5040/T$). (This is equivalent to assuming radiative equilibrium in the umbra.) We have computed models with $\Delta\theta = 0.1\ (0.1)\ 0.6$ using the opacity tables of Bode (1965). Some of these models are shown in Figure 8, and for comparison, the model of Kneer (1972) is also shown. Kneer's model is indistinguishable from the model $\Delta\theta = 0.4$ high in the atmosphere, where radiative equilibrium must exist. Deeper in the umbra, the departure from radiative equilibrium is due to the onset of convection.

For purposes of our Alfvén wave computations, the density scale heights are of interest (see Figure 9). In the solar model, the presence of a density inversion causes H_ρ to be a very irregular function of optical depth. Such behavior would greatly complicate the investigation of Alfvén wave

propagation. Fortunately, in the umbral models having $\Delta\theta \geq 0.3$, the irregularities disappear, and the density scale height now varies smoothly over the entire range of optical depths considered here. This is not to say however that irregularities would not be encountered at greater depths. In the solar model, the inversion coincides with the onset of hydrogen ionization, and in the umbral models, this is postponed to greater depths.

Unfortunately, no convergent solution has yet been found for the Alfvén wave flux. The above equation (3) includes only terms of first order in the wave amplitude. Second order terms have now been added, but the program is now so much more complicated that debugging has not yet been completed satisfactorily. At present, the solutions have not yet been obtained. Rotation of the plane of polarization of the wave must also be considered.

f. Magnetic Convection in the Sun and Solar Neutrinos

It was suggested by Schatten (1973) that magnetic fields inside the Sun might rise to the surface by buoyancy from the deep interior, thereby contributing to the transport of solar energy flux. He speculated that this might have a sufficiently large effect on the temperature structure of the sun that the neutrino flux emitted by the sun would become small enough to agree with observations. We have shown that this is very unlikely, for the velocities of upward motion of magnetic flux ropes in the radiative interior can be shown to be of order

0.01 cm/sec or less. Such small velocities cannot change the temperature structure by more than one part in 10^5. In particular, the central temperature will not change by more than a small fraction of 1%. Thus the effect of magnetic fields inside the sun can in all probability not contribute significantly to resolving the neutrino controversy.

g. Models of Starspots on Flare Stars

In last year's annual report, we described a model developed for sunspots based on the assumption that the missing flux was in the form of Alfvén waves (Mullan, 1974). The waves were assumed to be generated by convective gas motions, which occur with reduced efficiency in the presence of a vertical magnetic field. A quantitative estimate of the reduction in convective efficiency is incorporated by means of a physically meaningful modification of the cellular model of turbulent heat convection due to Öpik (1950; also Mullan, 1971). The model had led to results for sunspots which were in agreement with a variety of observations.

This model has now been extended to the case of cool spots on stars of late spectral type on the lower main sequence, and the results agree with observations very well. Further application of the starspot model to another class of stars will be described in the following section. Here we confine our remarks

to the flare stars.

The model in the case of sunspots had indicated that for field strengths less than a critical value B_c, no spot model was possible. This lower limit arises because for fields less than B_c, the field is strong enough to reduce the efficiency of convection appreciably, and yet not strong enough to compensate for the reduced convective flux by emitting sufficient Alfvén waves. Thus, flux constancy cannot be achieved unless $B > B_c \approx$ 1200 gauss in the sun. In a red dwarf of spectral type M0 ($T_{eff} = 4000^{\circ}K$), B_c was found to be much larger, of order B_c = 10-15 kilogauss. Hence starspots on red dwarfs require much stronger fields than sunspots. However, the fields cannot become too strong, for then the Wilson depression exceeds 1000 km and the spot would be washed out rapidly by radiative heating across the walls of the spot. This sets an upper limit of 30-40 kilogauss on the field strengths in starspots. A typical surface field strength of a starspot on an M0 star (with mass $\approx 0.6\ M_{\odot}$) is therefore about 20 kilogauss.

Independent estimates of field strength in such a star can be derived from flare energies and from the general properties of the variation of pressure with depth. These both lead to estimates of field strengths in agreement with the above estimate. More recently, in considering the evolution of stellar dynamos, we have in a completely independent way verified that fields

of order 20 kilogauss are to be expected in starspots on stars with $M = 0.6\ M_{\odot}$.

With a surface field of 2×10^4 gauss, it is necessary to incorporate a field gradient so that the field becomes stronger inside the star, and makes the starspot as deep as the convection zone. It is a postulate of our model (Mullan 1973) that a spot is a special kind of convection cell which penetrates to the base of the convection zone, and has a diameter, D, which is simply proportional to the depth of the convective zone, H. The constant of proportionality, D/H, can be estimated for polytropic models, and in the case of the sun, D/H varies from 2 to about 7, with preferred values apparently at 2.9 and 5.4 (cf. Bumba, Ranzinger and Suda, 1973, especially their Figure 7, and note that we have taken the depth of the solar convection zone to be 10^4 km, following Mullan, 1971). This leads us then to expect that in stars of later spectral types, where the convection zone occupies an increasingly large fraction of the radius of the star (see Figure 10), the fraction of the surface area occupied by a spot must increase. In fact, in the cases of the stars YY Gem, CC Eri and BY Dra, the sizes of the starspots (Bopp and Evans, 1973; Bopp, 1974) are consistent with our hypothesis if D/H = 3, 3, and 5 respectively. These are close to the preferred solar ratios of 2.9 and 5.4, and this gives us some confidence that our postulate of D proportional to H is

acceptable. Further confirmation of this postulate will appear in the following section.

Once the field strength is known at the surface, and a gradient has been chosen, the computation of a spot model proceeds as for the sunspot case, except that the condition of equal gas density inside and outside the spot has been relaxed. Results are indicated in Figure 11. The effective temperature of the spot at the surface turns out to be very low, about 1600°K. Bopp and Evans (1973) had suggested that the effective temperature in spots observed by them might be about 2000°K, but this number is extremely uncertain, and the good agreement with the umbral surface effective temperature deduced here must be considered coincidental.

h. Starspots on the Primaries of Contact Binary Systems

Further application of our starspot models is now possible in the case of W Ursae Majoris type binaries. These binaries are considered to be encompassed by a common convective envelope which has the result of equalizing the entropy in each component's convection zone (Lucy, 1968) with the result that effective temperatures of both primary and secondary components become equal. Observations of hotter W UMa systems (the so-called A-type systems) indicate that the two components do indeed have closely equal effective temperatures. On the other

hand, the cooler systems (called W-types) are observed to have temperature differences between primary and secondary, ΔT, which are of order several hundred degrees. In terms of the parameter $X = \Delta T/T$, the observations suggest that X ranges from 0.02 to 0.11-0.13 in different W UMa systems.

It is possible to interpret these X-values in terms of starspots on the primary if the spots have diameters proportional to the depth of the convection zone. The preferred values $D/H = 2.9$ and 5.4 lead to theoretical values of X as a function of stellar B-V color as shown in Figure 12. Points denote observed values. It seems that our starspot postulate leads to a very plausible interpretation of the photometric peculiarities of the W-type systems.

The presence of spots causes distortions of the light curves, and we have obtained quantitative agreement (to accuracies of $0^{m}.02$) between predicted and observed distortions in four systems.

The W UMa systems are especially suited for stellar dynamo activity on account of the simultaneous occurrence of deep convection zones and rapid rotation. The latter is enforced by tidal effects.

i. Implications of Starspots on Red Dwarfs

If the fields in starspots on red dwarfs are indeed as large as 20 kilogauss, then fields in active regions around such spots must also be much larger than in the sun. This leads us to expect that hydromagnetic heating of chromospheres in magnetic red dwarfs must be about two orders of magnitude greater than in the sun. We believe that this explains why chromospheres of dMe stars are 10-100 times denser than in the sun.

Such dense chromosphere-coronas also lead us to expect that analogous to the Moreton waves which are emitted following certain large solar flares, and which may trigger sympathetic flares in distant active regions, stellar flares also emit Moreton waves which travel with speeds roughly equal to those observed in the sun.

Starspots have effective temperatures which are so cool that grains in all likelihood can condense. If dMe stars have dense chromospheres because of strong magnetic activity, then grains should form in dMe stars following starspot activity. However, dM stars presumably have no magnetic activity, and so grains would not be formed. We believe that it is grains in dMe circumstellar shells which causes the slight systematic infrared excess of dMe stars relative to dM stars.

A point of major interest in stellar chromospheres is the question of possible cyclic activity. No such cycles have yet been definitely determined. We believe that this is due to the

long lifetime of starspots on these stars. Vogt (1973) has found that a spot on BY Dra has survived as long as eight years. If starspots survive longer than the period of the magnetic cycle, it will be very difficult to discover cyclic behavior. On the basis of a numerical model of the evolution of stellar dynamos in red dwarfs, we believe that the cycle time in red dwarfs may in fact be quite short, or order 1-3 years, and therefore much shorter than the lifetime of starspots.

The release of energy in stellar flares can be on a much grander scale than in solar flares. Thus 7×10^{34} ergs of radiative energy was released in a flare of YZ CMi (Kunkel, 1969). This exceeds the largest solar flare by a factor of almost 10^3. It is hoped that an understanding of the relation of starspots and stellar flare may help to understand the relation between sunspots and solar flares, and vice versa.

IV. Personnel Activities

Paper Presentations and Meeting Attendance

"Observations of the Sun", by D.J. Mullan, colloquium talk at the Physics Department, Lycoming College, Williamsport, Pennsylvania, November 23, 1973.

"Starspots on Red Dwarfs", by D.J. Mullan, colloquium talk at the Astronomy Departmen University of Texas at Austin, April 22, 1974.

"Magnetic Fields in the Sun", by D.J. Mullan, invited paper at a symposium commemorating the 50th Anniversary of Bartol Research Foundation, May 11, 1974.

"Magnetic Fields on Spotted Red Dwarfs", by D.J. Mullan, paper presented at the 143rd Meeting of the American Astronomical Society in Rochester, New York, August 23, 1974.

Papers Published

"Flare Triggering by Coherent Oscillations", by D.J. Mullan, Astrophysical Journal 185, 353, 1973.

"Sunspots, Supergranules, and the Depth of the Solar Convection Zone", by D.J. Mullan, Astrophysical Journal 186, 1059, 1973.

"Sunspot Models with Alfvén Wave Emission", by D.J. Mullan, Astrophysical Journal, 187, 621, 1974.

"Starspots on Flare Stars", by D.J. Mullan, Astrophysical Journal, 192, 149, 1974.

"Correction of Sunspot Intensities for Scattered Light", by D.J. Mullan, Solar Physics 32, 65, 1973.

"Comments on Papers by P.R. Wilson Concerning Sunspots", by D.J. Mullan, Solar Physics 32, 441, 1973.

"Fast Rotation of Metal Poor Stars", by D.J. Mullan, Astronomy and Astrophysics 27, 379, 1973.

"Magnetic Fields on Spotted Red Dwarfs", by D.J. Mullan, Bulletin of the American Astronomical Society, 6, 333, 1974.

Papers in Press

"Magnetic Fields in the Sun", by D.J. Mullan, Journal of the Franklin Institute.

"Magnetic Convection in the Sun", by D.J. Mullan, Solar Physics.

Papers Submitted for Publication

"Magnetic Fields and Dense Chromospheres in dMe Stars", by D.J. Mullan, Astrophysical Journal.

"On the Possibility of Magnetic Starspots on the Primary Components of W Ursae Majoris Type Binaries", by D.J. Mullan, Astrophysical Journal.

Personnel Changes

Dr. Arne A. Wyller left Bartol to take up responsibilities as Research Professor and Director of the Swedish Astrophysical Observatory at Anacapri, Italy.

During July and August 1974, an undergraduate summer student, John Oliensis, of Yale University, contributed to the theoretical work on Alfvén wave propagation.

Dr. D.J. Mullan has continued full-time work on both the observations and theoretical aspects of sunspots and starspots.

V. References

Alfvén, H. and Fälthammer, C.-G., 1963, Cosmic Electrodynamics (Oxford: Clarendon Press) p. 86.

Bahng, J. and Schwartschild, M., 1961, Astrophys. J. 134, 338.

Baker, N.H. and Temesvary, S., 1966, Tables of Convective Stellar Models (2nd Edition), published by NASA Goddard Institute for Space Studies, New York.

Beckers, J., 1969, Solar Phys. 9, 372.

Bode, G., 1965, Continuous Absorption Coefficients as Functions of Pressure, Temperature and Chemical Composition, (Kiel: Institute of Theoretical Physics).

Boole, E., 1844, Phil. Trans. Roy. Soc. p. 239.

Bopp, B.W., 1973, Bull. Amer. Astron. Soc. 5, 399.

Bopp, B.W. and Evans, D.S., 1973, Monthly Notices Roy. Astron. Soc. 164, 343.

Borra, E.F., Landstreet, J.D. and Vaughan, A.H., 1973, Astrophys. J. Letters, 185, L145.

Branch, D., 1970, Astrophys. J. 159, 39.

Bray, R.J. and Loughhead, R.E., 1964, Sunspots (London: Chapman and Hall).

Bumba, V., Rarzinger, P. and Suda, J., 1973, Bull. Astron. Inst. Czecho. 24, 22.

Chisnell, R.F., 1955, Proc. Roy. Soc. London A232, 350.

Copeland, H., Jensen, J.O. and Jorgensen, H.E., 1970, Astron. Astrophys. 5, 12.

Cowling, T.G., 1953, The Sun, ed. G.P. Kuiper (Chicago Univ. Press) p. 549.

Danielson, R.E., 1973, private communication.

Danielson, R.E. and Savage, B.D., 1968, Structure and Development of Active Regions, ed. K.D. Kiepenheuer (Dordrecht: D. Reidel Publ. Co.), p. 112.

Deift, P.A. and Goertz, C.K., 1973, Planetary and Space Science, 21, 1417.

Ekmann, G. and Mattby P., 1974, Solar Phys. 35, 317.

Ferraro, V.C.A., 1954, Astrophysical J. 119, 393.

Ferraro, V.C.A. and Plumpton, C., 1958, Astrophysical J. 127, 459.

Frisch, U., 1964, Annales d'Astrophysique 27, 224.

Gingerich, D. and de Jager, C., 1968, Solar Phys. 3, 5.

Hencux, J.C., 1969, Astron. Astrophys. 2, 288.

Hollweg, J.V., 1972, Cosmic Electrodynamics, 2, 423.

Ingersoll, L.R., Adler, F.T., Plass, H.J. and Ingersoll, A.C. 1950, Heating, Piping, and Air Conditioning, 22, 113.

Johnson, H.L., 1966, Ann. Rev. Astron. Astrophys. 4, 193.

Jordan, S., 1970, Astrophys. J. 161, 1189.

Kneer, F., 1972, Astron. Astrophys. 18, 39.

Koch, R.H., 1974, Astron. J. 79, 34.

Kunkel, W.E., 1969, Nature 222, 1129.

Landau, L.D. and Lifshitz, E.M., 1959, Fluid Mechanics,
(Reading, Mass.: Addison-Wesley) p. 303.

Lucy, L.B., 1968, Astrophys. J. 151, 1123.
Marik, M., 1967, Soviet Astronomy A.J. 11, 264.
Mauder, H., 1972, Astron. Astrophys. 17, 1.

Mihalas, D., 1967, in Methods in Computational Physics, ed.
B. Alden, S. Fernbach and M. Rotenberg (New York:
Academic Press), p. 1.

Miller, R.A., 1974, Solar Phys. 36, 91.

Mullan, D.J., 1971, Monthly Notices Roy. Astron. Soc. 154, 467.

Mullan, D.J., 1972, Nature Phys. Sci. 235, 58.

Mullan, D.J., 1973, Astrophys. J. 186, 1059.

Mullan, D.J., 1974, Astrophys. J. 187, 621.

Opik, E.J., 1950, Monthly Notices Roy Astron. Soc. 110, 559.

Osterbrock, D.E., 1961. Astrophys. J. 134, 347.

Pikelner, S.B. and Livshits, M.A., 1965, Soviet Astronomy A.J.
8, 808.

Rossbach A. and Schröter, E.H., 1970, Solar Phys. 12, 95.

Rucinski, S.M., 1974, Acta Astronomica 24, Number 2 (in press).

Schatten, K.H., 1973, Solar Phys. 33, 305.

Stein, R.F., 1971, Astrophys. J. Suppl. 22, 419.

Stellmacher, G. and Wiehr, E., 1972, Astron. Astrophys. 19, 293.

Straka, W.C., 1971, Astrophys. J. 165, 109.

Unno W., 1956, Public Astron. Soc. Japan 8, 108.

Vogt, S.S., 1973, Bull. Amer. Astron. Soc. 5, 399.

"
Wohl, H., 1970, Solar Phys. 15, 338.

Yun, H.S., 1970, Astrophys. J. 162, 875.

Yun, H.S., 1971, Solar Phys. 16, 379.

Zwaan, C., 1965, Recherches Astron. Obs. Utrecht, XVII, p. 1

Zwaan, C., 1968, Ann. Rev. Astron. Astrophys. 6, 135.

Zwaan, C., 1974, Solar Phys. 37, 99.

Captions for Figures

Fig. 1 Idealized spectrum of spot near the sodium D lines, indicating the intensities involved in defining a two-dimensional classification of sunspot atmospheres. ⊗ denotes continuum windows in sunspot spectra, following Wöhl (1970). I_A is the interpolated continuum intensity in the spot at 5893.4Å. I_B is the actual measured intensity in the spot at 5893.4Å. The classification suggested here is $r_{spot} = I_B\,(spot)/I_A(spot)$ and $R_{spot} = I_A(spot)/I_A(sun)$.

Fig. 2 Two-dimensional classification of the line-and continuum-forming regions in sunspot atmospheres. See legend of Figure 1 for definitions of r_{spot} and R_{spot}. Observations are characterized by lines, indicating the date of observation, the umbral area in millionths of a solar hemisphere, and the minimum Z correction factor for scattered light. Note that errors due to scattered light lead to sloping lines in this figure, rather than error boxes. Theoretical model predictions at disk center are indicated by enclosed letters (K = Kneer (1972); SW = Stellmacher and Wiehr (1972); Y = Yun (1971); YI, YII = revised models of Yun). Two observations with large r_{spot} (> 0.9) are near the limb, where theoretical models predict larger r_{spot} values.

Fig. 3 Broad-band intensity of spots expressed in terms of the disk intensity. Four filters were used on October 24, 1973, seven on October 26, 1972. Solid lines are theoretical model predictions of continuum intensity. The large uncertainty at 4200Å is due to uncertainties in correction for line blanketing in the spot. It is unlikely that errors in observations and reduction can account for the large differences between the two spots. The larger umbra appears to be definitely darker than the smaller umbra.

Fig. 4 Dots represent counting rates per second N as a function of position as the telescope is stepped in 2" steps north of the center of the umbra. At the center of the umbra (point labelled C) the counting rate is 206 thousand photons/sec. The line ED is an eye-fitted line through the observations, indicating the decrease in intensity away from the spot. The undisturbed disk intensity corresponds to a counting rate of 470 thousand photons/sec, although limb darkening needs to be taken into account across the scan. The missing flux in the spot may have reappeared as the excess (denoted by line ED) of intensity above the undisturbed intensity (denoted by BD).

Fig. 5 Function G(z,p) appearing in the solution for heat conduction outside a cylinder of radius a. Curves have been drawn through values tabulated by Ingersoll et al. (1950) for the case when a constant heat flux emerges across the curved surface of the cylinder. At a given time, excess temperature at radius r outside the cylinder is proportional to G evaluated at p = r/a along a vertical line of constant z. At a given position outside the cylinder (constant p), the excess temperature grows asymptotically as log (time).

Fig. 6 T = Ratio of transmitted flux to incident flux when Alfvén waves impinge on a discontinuity where density decreases from ρ_1 to ρ_2. Solid curve is the function derived by (e.g.) Alfvén and Fälthammar (1963). The dash-dot curve is the approximation used by Pikelner and Livshits (1965) for Alfvén waves; the dotted line is their approximation for fast-mode waves. In the WKB approximation (wavelength much less than density scale height) the flux of waves transmitted through a region where density declines gradually from ρ_1 to ρ_2 remains equal to unity (dashed curve). The arrows denote special case of waves propagating between the bottom and the top of the solar convection zone.

Fig. 7 Flux of Alfvén waves as function of height above Wilson depression. Solution is obtained by numerical integration of equation (3) at fixed radius, assuming that the field geometry in the spot is that of Yun (1970). Numerical errors, or incorrect approximations, or both, may be responsible for the unphysical behavior of the solution in those regions where the Alfvén wave flux exceeds the total solar flux.

Fig. 8 Temperature structure of umbral models computed according to the method of Mihalas (1967). The temperatures in the umbra differ from the solar temperatures at equal optical depth by an amount $\Delta\theta$ = constant. The umbral model atmosphere of Kneer (1972) is shown for comparison.

Fig. 9 Density scale height as a function of depth in the umbral atmosphere models. Irregularities in the solar model are caused by a density inversion in the HSRA model.

Fig. 10 Depth of convection zones in stars on the lower main sequence. Depth is expressed in terms of the stellar radius; abscissa is mass in units of the solar mass. Results for $M/M_\odot \geq 0.4$ are taken from Copeland *et al.* (1970). Completely convective stars set in at $M/M_\odot = 0.3$ (Copeland *et al.*) or at $M/M_\odot = 0.20$ (Straka 197[illegible].

Fig. 11 Physical variables in a model of a starspot on YY Gem as a function of depth. The depth is expressed both in terms of the gas pressure in the undisturbed stellar model and in terms of the depth Z(cm). B is magnetic field strength; D/H is the local ratio of convective cell diameter to cell depth; T_e is the local effective temperature in the spot, defined such that the local sum of radiative plus convective fluxes equals σT_e^4, where σ is the Stefan-Boltzmann constant. Some of the fluctuations in T_e are due to numerical errors when the temperature gradient is very close to adiabatic. NE denotes the range of depths in the model where numerical errors are so severe that there occurs an apparent suppression of convection altogether. This is not considered to be physically meaningful. However, the decrease in T_e near the surface is real.

Fig. 12 Effect of a starspot on effective temperature of main sequence stars. The curves are theoretical estimates, μ, of the decrease in the mean effective temperature of the visible disk of the primary component when a starspot is fully visible on the disk. Spot diameter D is assumed to be proportional to depth of convection zone H. Numerical values of H (Copeland et al, 1970)

are obtained here by assuming that B-V is convertible to T_e using Johnson's (1966) tables. Observed values of $X = \Delta T/T$ for individual W UMa systems are taken from Table 2 of Rucinski (1974). Colors are taken from Mauder (●; 1972) and Koch (o; 1974). Temperature of spot varies with stellar temperature (see text). Numbers beside tick marks on each curve are magnitudes of fading in visual light caused by the spot if it existed on a single star. In a close binary, the total light will fade by a smaller amount.

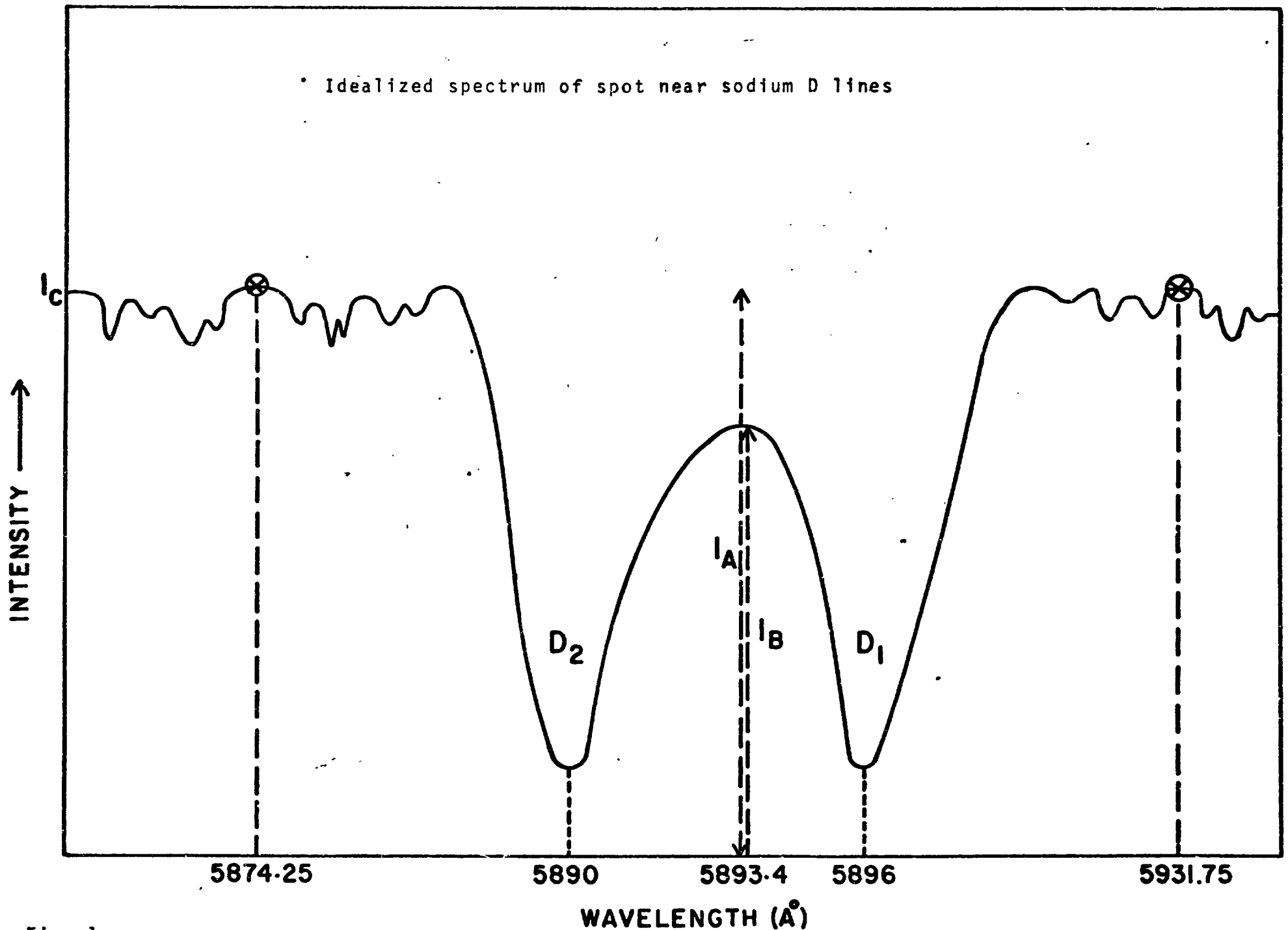
Idealized spectrum of spot near sodium D lines
I_C
INTENSITY
I_A
I_B
D_2
D_1
5874·25
5890
5893·4
5896
5931.75
WAVELENGTH (Å)

Fig. 1

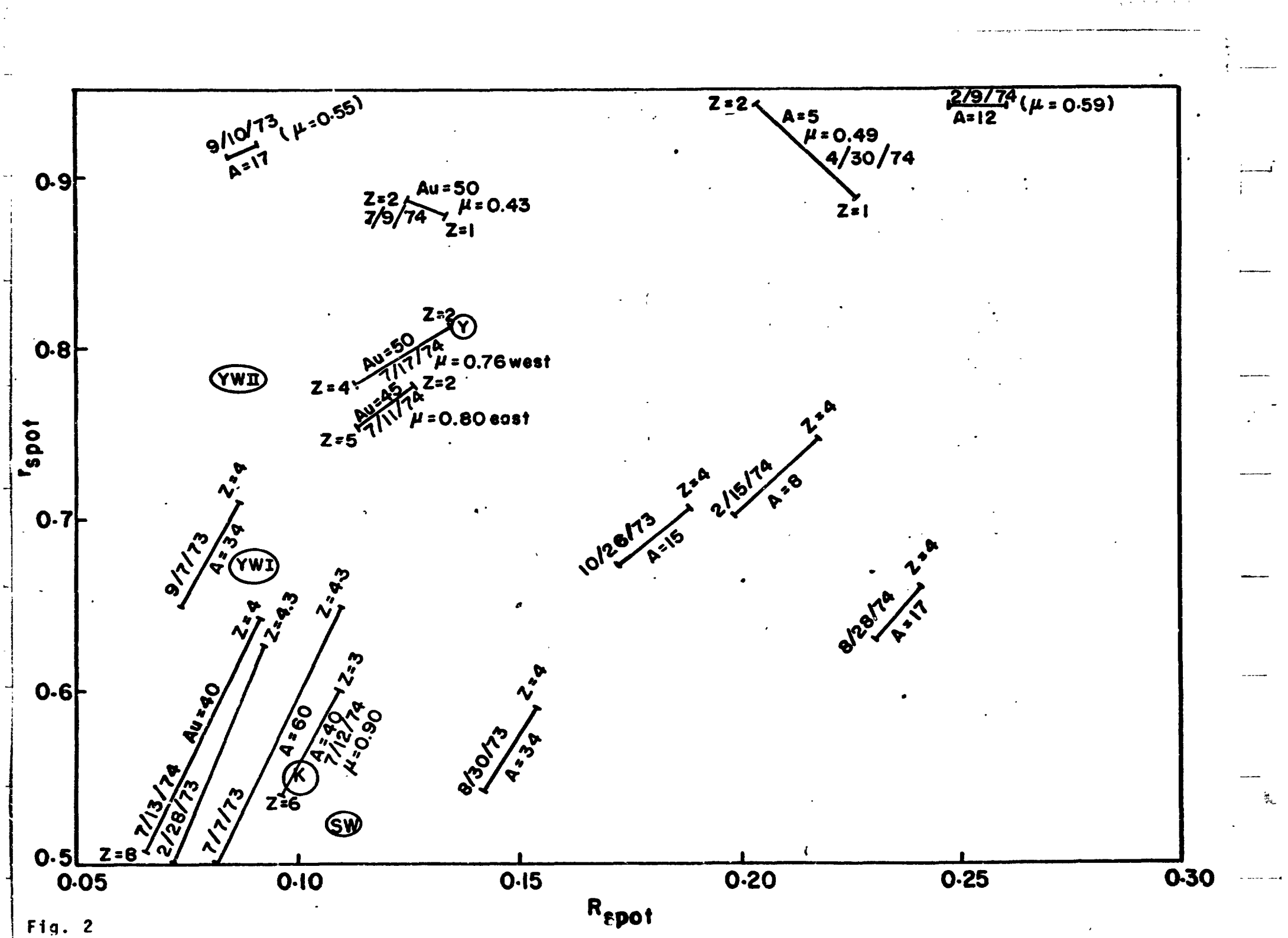
9/10/73
A=17
(μ=0.55)
Z=2
A=5
μ=0.49
4/30/74
Z=1
2/9/74
A=12
(μ=0.59)
Z=2
7/9/74
Au=50
μ=0.43
Z=1
Z=2
Y
Au=50
7/17/74
μ=0.76 west
Z=4
YWII
Au=45
7/11/74
Z=2
μ=0.80 east
Z=5
Z=4
9/7/73
A=34
YWI
Z=4
10/26/73
A=15
Z=4
2/15/74
A=8
Z=4
8/28/74
A=17
Z=4
Z=4.3
Z=4.3
Au=40
7/13/74
2/28/73
7/7/73
Z=8
A=60
Z=3
A=40
7/12/74
μ=0.90
T
Z=6
SW
8/30/73
A=34
Z=4
0.9
0.8
0.7
0.6
0.5
r spot
0.05
0.10
0.15
0.20
0.25
0.30
R spot

Fig. 2

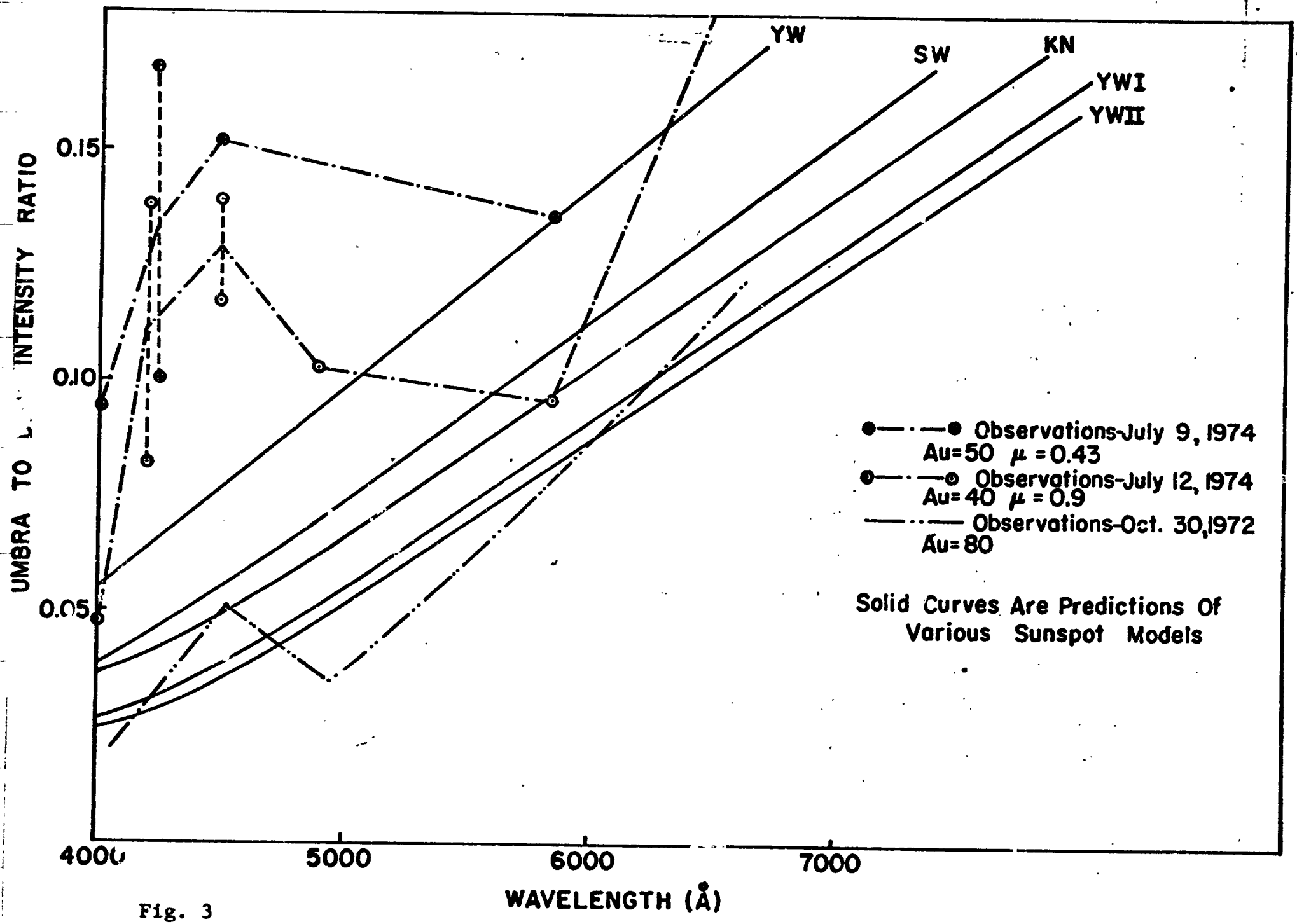
YW
SW
KN
YWI
YWII
0.15
0.10
0.05
UMBRA TO
INTENSITY RATIO
4000
5000
6000
7000
WAVELENGTH (Å)
Observations-July 9, 1974
Au=50 μ = 0.43
Observations-July 12, 1974
Au=40 μ = 0.9
Observations-Oct. 30,1972
Au=80
Solid Curves Are Predictions Of
Various Sunspot Models

Fig. 3

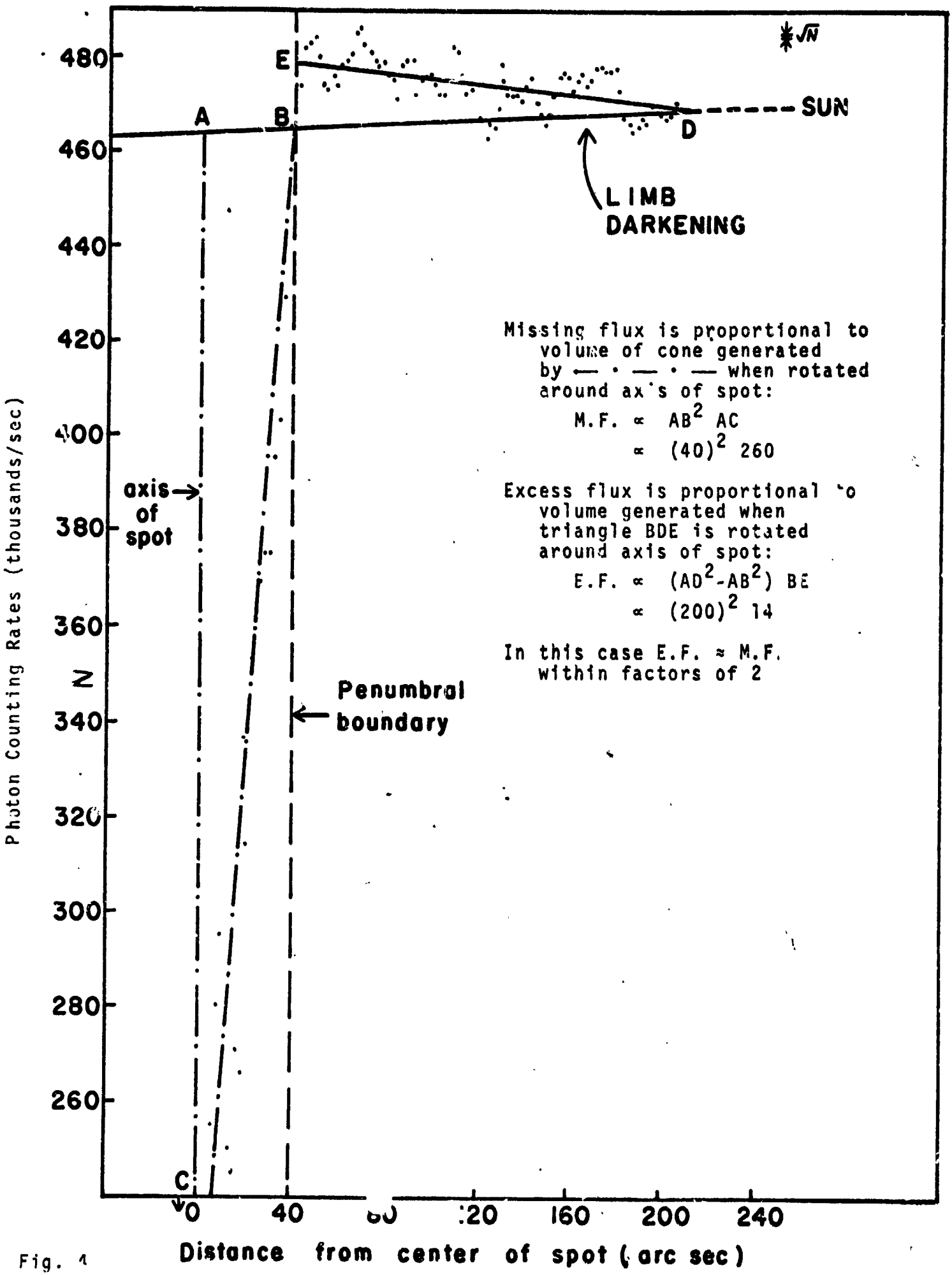
480
460
440
420
400
380
360
340
320
300
280
260
N
Photon Counting Rates (thousands/sec)
E
A
B
D
SUN
LIMB DARKENING
√N
axis of spot
Penumbral boundary
C
0
40
80
120
160
200
240
Distance from center of spot (arc sec)
Missing flux is proportional to volume of cone generated by — · — · — when rotated around axis of spot:
M.F. ∝ AB² AC
∝ (40)² 260
Excess flux is proportional to volume generated when triangle BDE is rotated around axis of spot:
E.F. ∝ (AD²-AB²) BE
∝ (200)² 14
In this case E.F. ≈ M.F. within factors of 2

Fig. 1

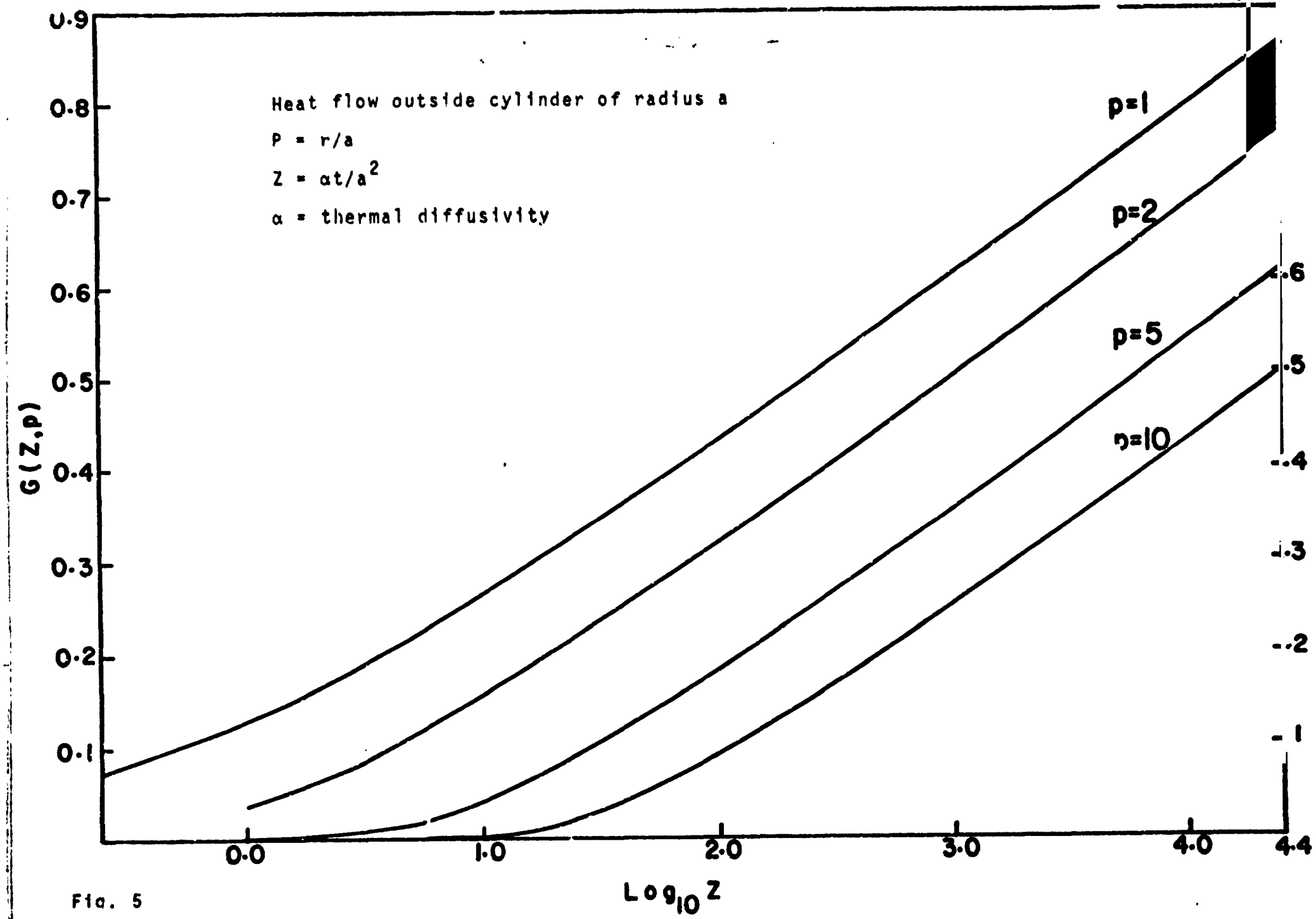
Heat flow outside cylinder of radius a
P = r/a
Z = αt/a²
α = thermal diffusivity
p=1
p=2
p=5
p=10
G(Z,p)
Log₁₀ Z
0.9
0.8
0.7
0.6
0.5
0.4
0.3
0.2
0.1
0.0
1.0
2.0
3.0
4.0
4.4
.6
.5
.4
.3
.2
1

Fig. 5

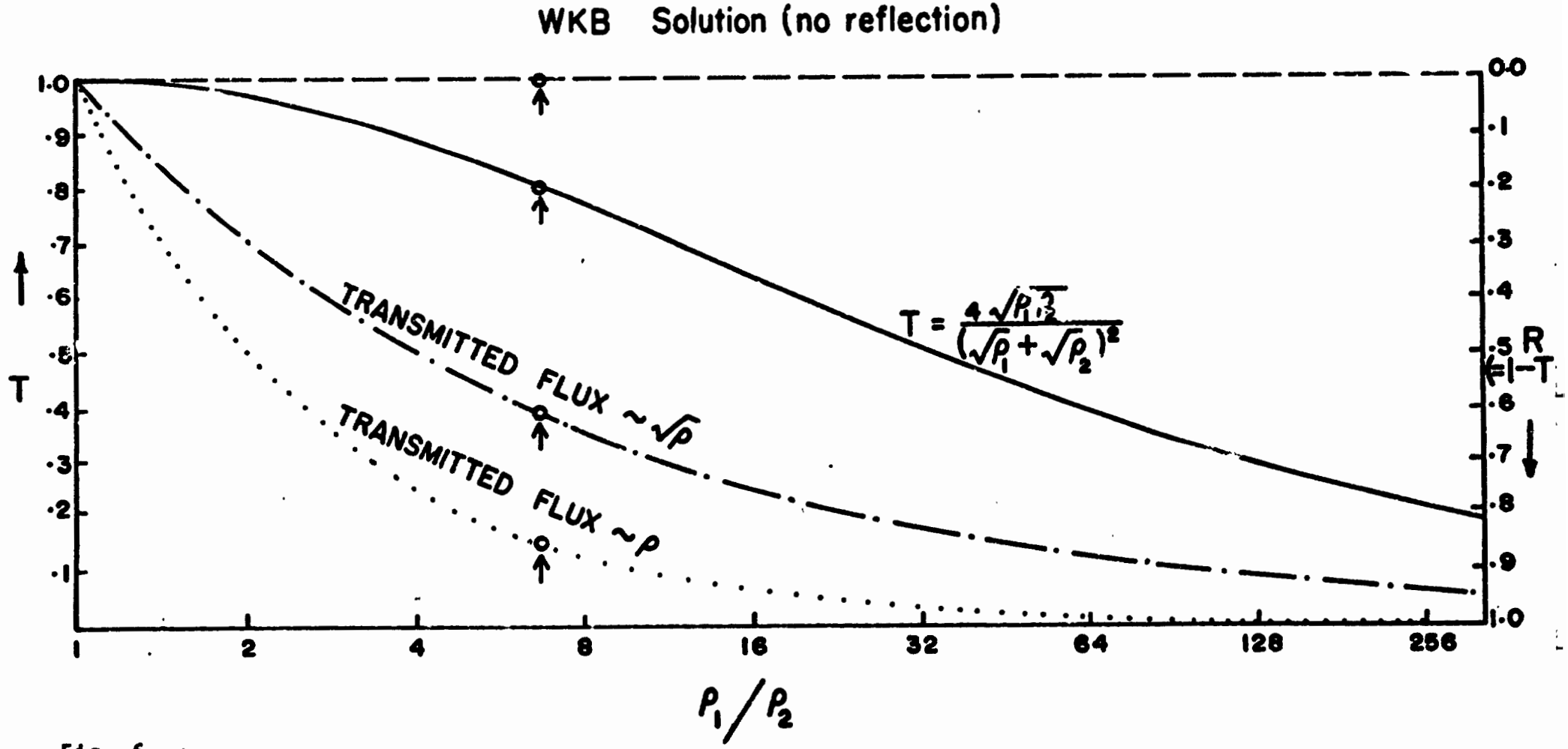
WKB Solution (no reflection)
T
R = 1 − T
TRANSMITTED FLUX ~ √ρ
TRANSMITTED FLUX ~ ρ
T = 4√(ρ1ρ2) / (√ρ1 + √ρ2)²
ρ1 / ρ2
1.0
.9
.8
.7
.6
.5
.4
.3
.2
.1
0.0
.1
.2
.3
.4
.5
.6
.7
.8
.9
1.0
1
2
4
8
16
32
64
128
256

Fig. 6

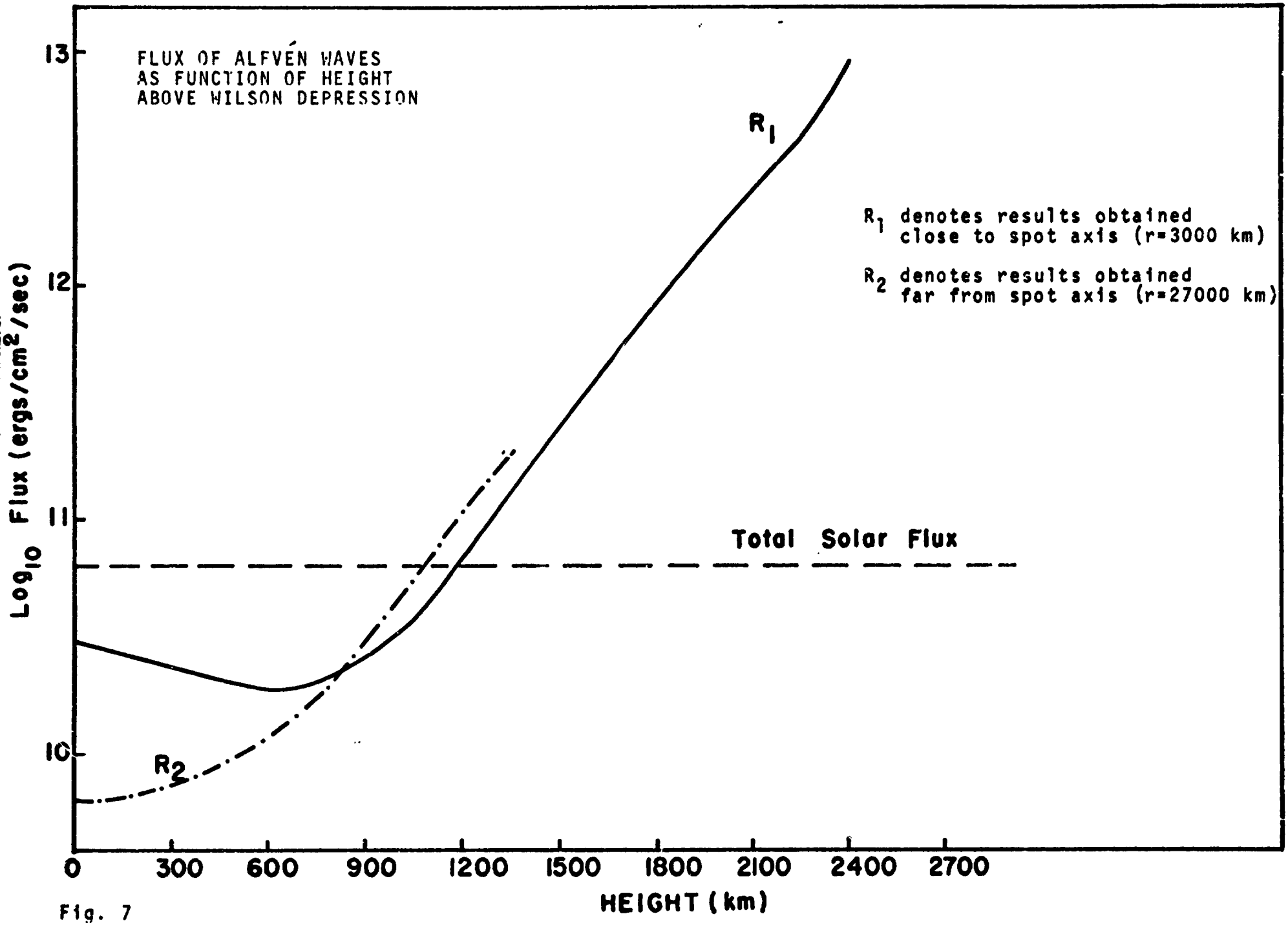
FLUX OF ALFVÉN WAVES
AS FUNCTION OF HEIGHT
ABOVE WILSON DEPRESSION
R1
R1 denotes results obtained close to spot axis (r=3000 km)
R2 denotes results obtained far from spot axis (r=27000 km)
Total Solar Flux
R2
13
12
11
10
Log10 Flux (ergs/cm2/sec)
0
300
600
900
1200
1500
1800
2100
2400
2700
HEIGHT (km)

Fig. 7

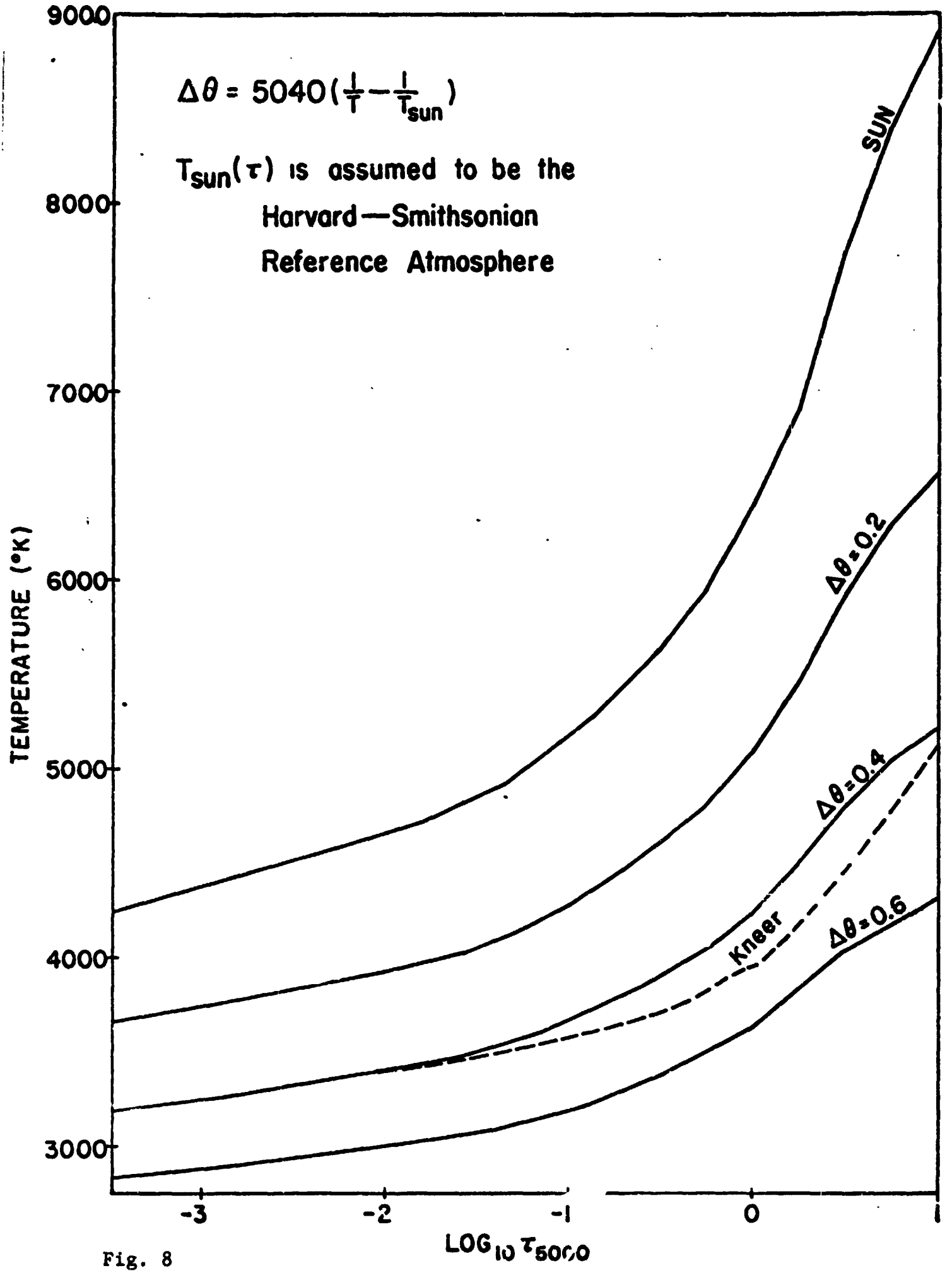
$\Delta\theta = 5040(\frac{1}{T} - \frac{1}{T_{sun}})$
$T_{sun}(\tau)$ is assumed to be the Harvard—Smithsonian Reference Atmosphere
SUN
$\Delta\theta$=0.2
$\Delta\theta$=0.4
Kneer
$\Delta\theta$=0.6
TEMPERATURE (°K)
9000
8000
7000
6000
5000
4000
3000
-3
-2
-1
0
1
$LOG_{10}\tau_{5000}$

Fig. 8

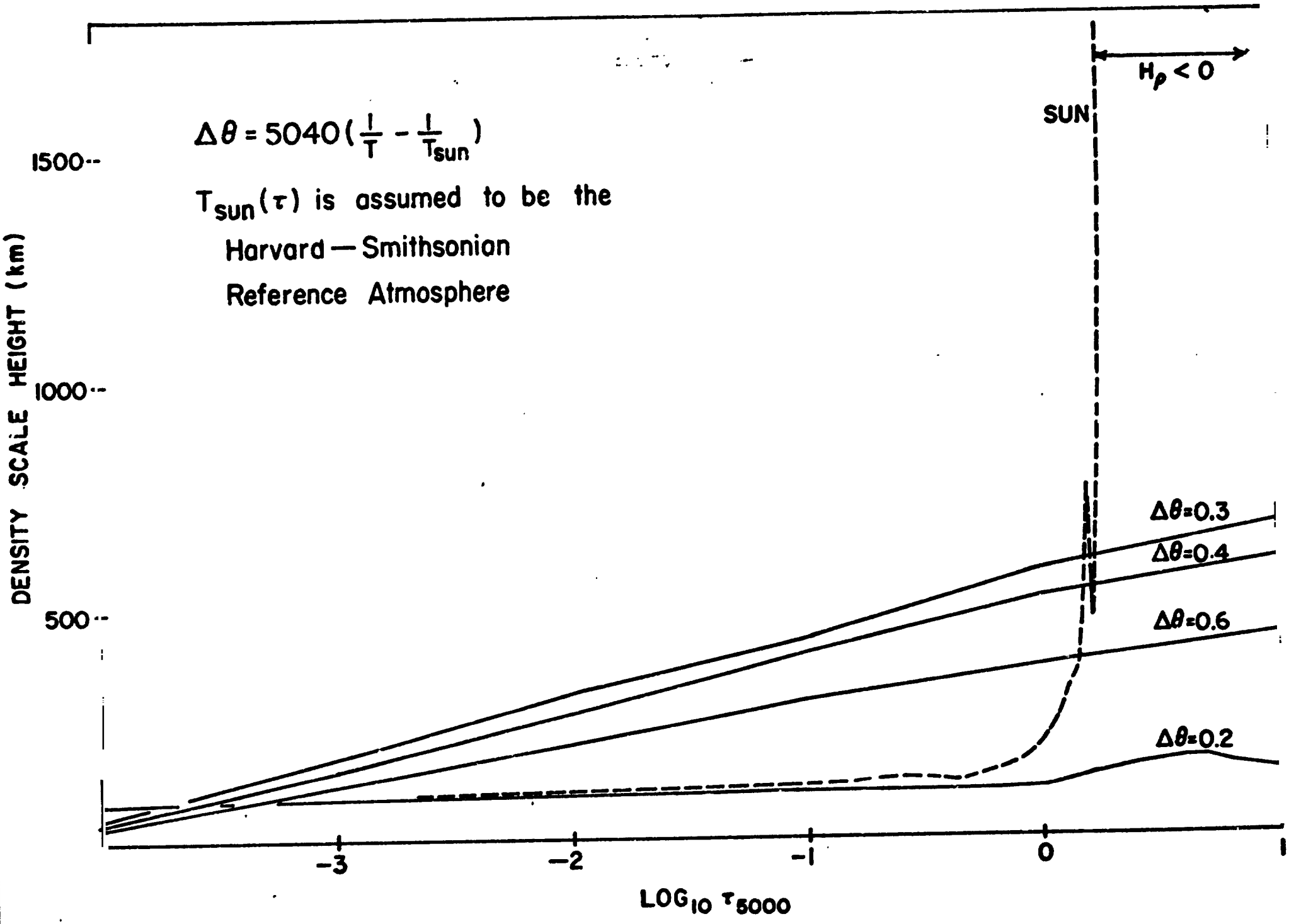
$\Delta\theta = 5040\left(\frac{1}{T} - \frac{1}{T_{sun}}\right)$
$T_{sun}(\tau)$ is assumed to be the Harvard — Smithsonian Reference Atmosphere
$H_\rho < 0$
SUN
1500
1000
500
DENSITY SCALE HEIGHT (km)
$\Delta\theta$=0.3
$\Delta\theta$=0.4
$\Delta\theta$=0.6
$\Delta\theta$=0.2
-3
-2
-1
0
1
$LOG_{10}\ \tau_{5000}$

Fig. 9

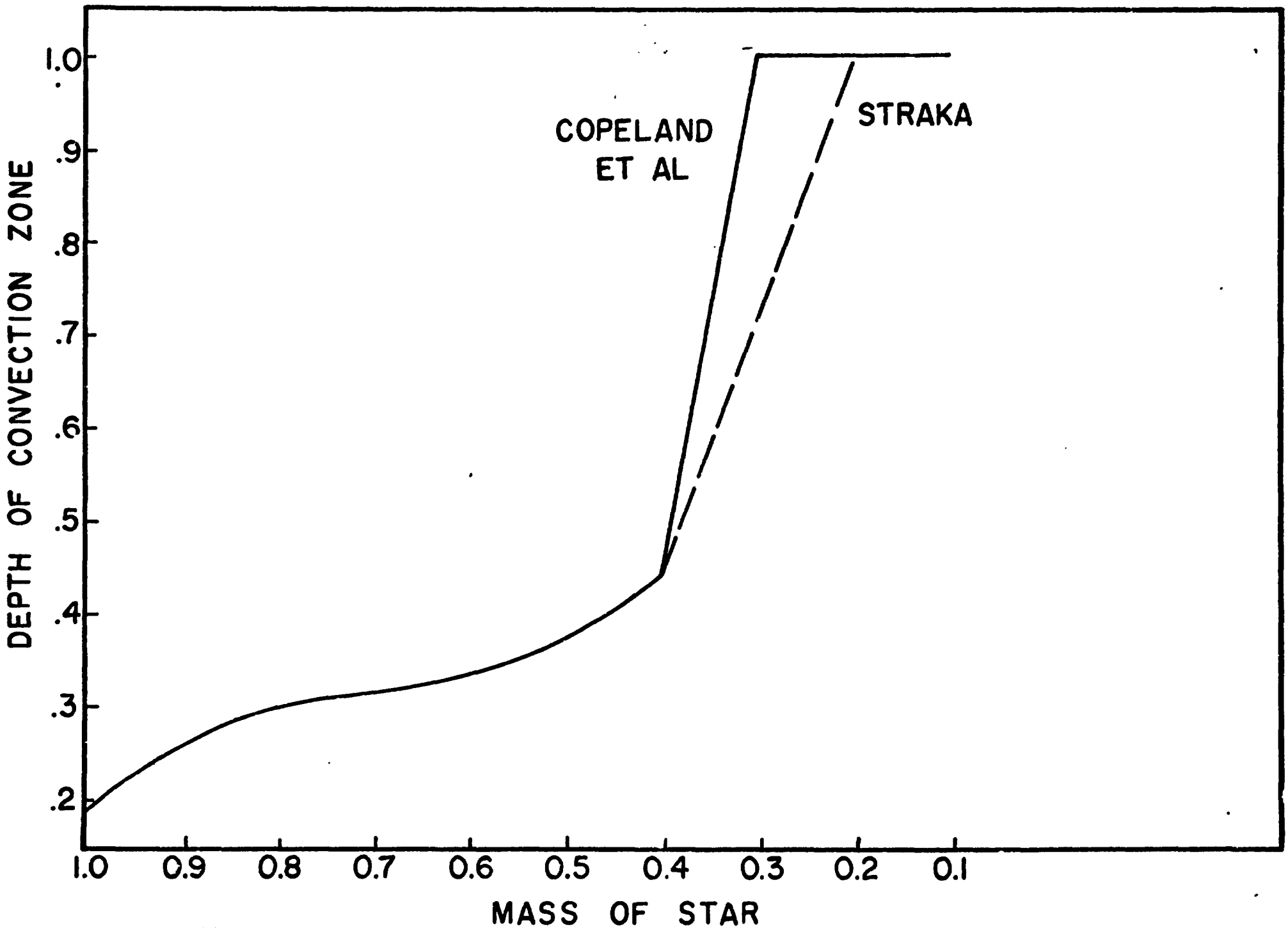
DEPTH OF CONVECTION ZONE
1.0
.9
.8
.7
.6
.5
.4
.3
.2
COPELAND
ET AL
STRAKA
1.0
0.9
0.8
0.7
0.6
0.5
0.4
0.3
0.2
0.1
MASS OF STAR

Fig. 10

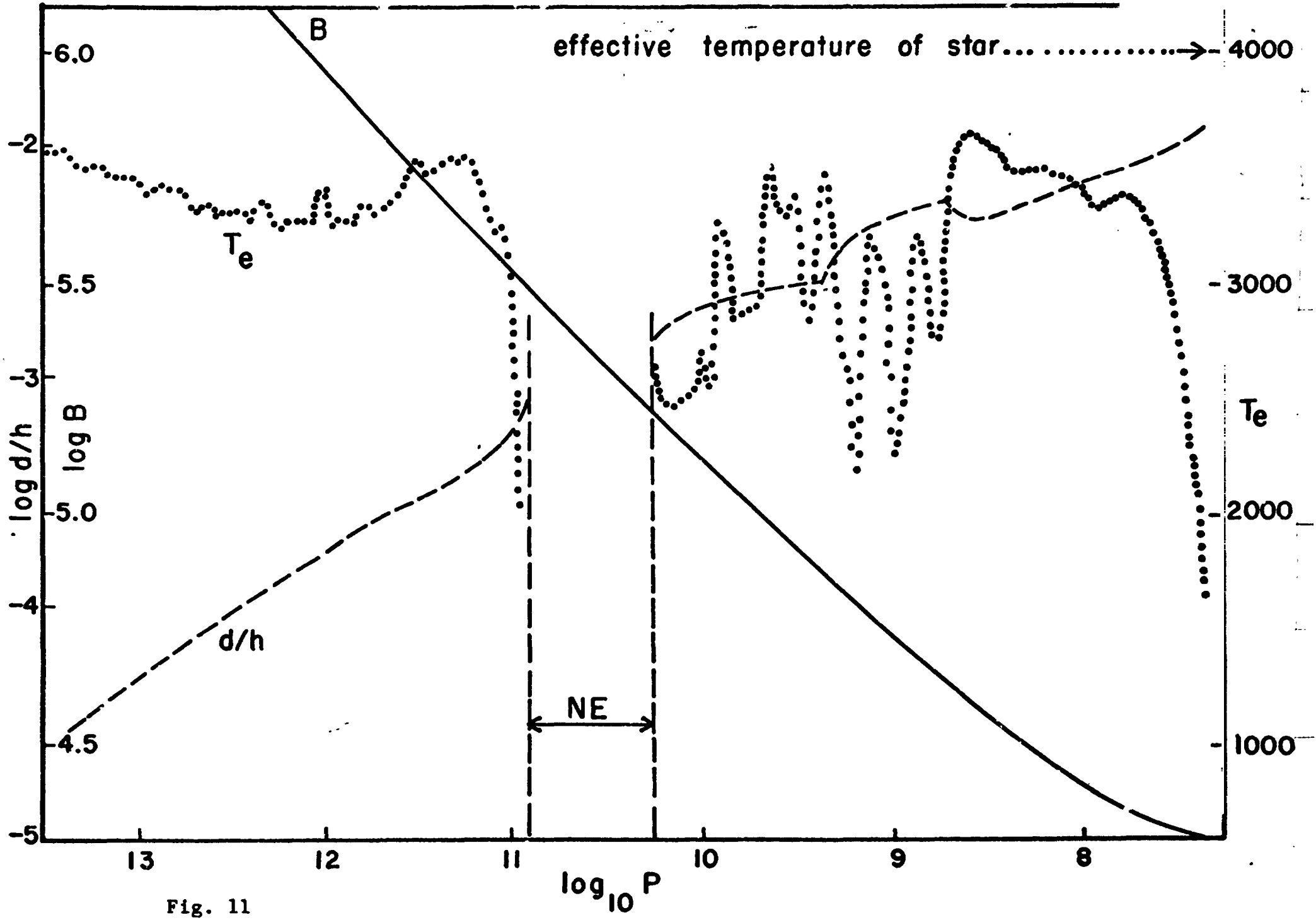
B
effective temperature of star.....→
6.0
-2
5.5
-3
5.0
-4
4.5
-5
T_e
d/h
log d/h
log B
NE
13
12
11
10
9
8
$\log_{10} P$
4000
3000
2000
1000
Te

Fig. 11

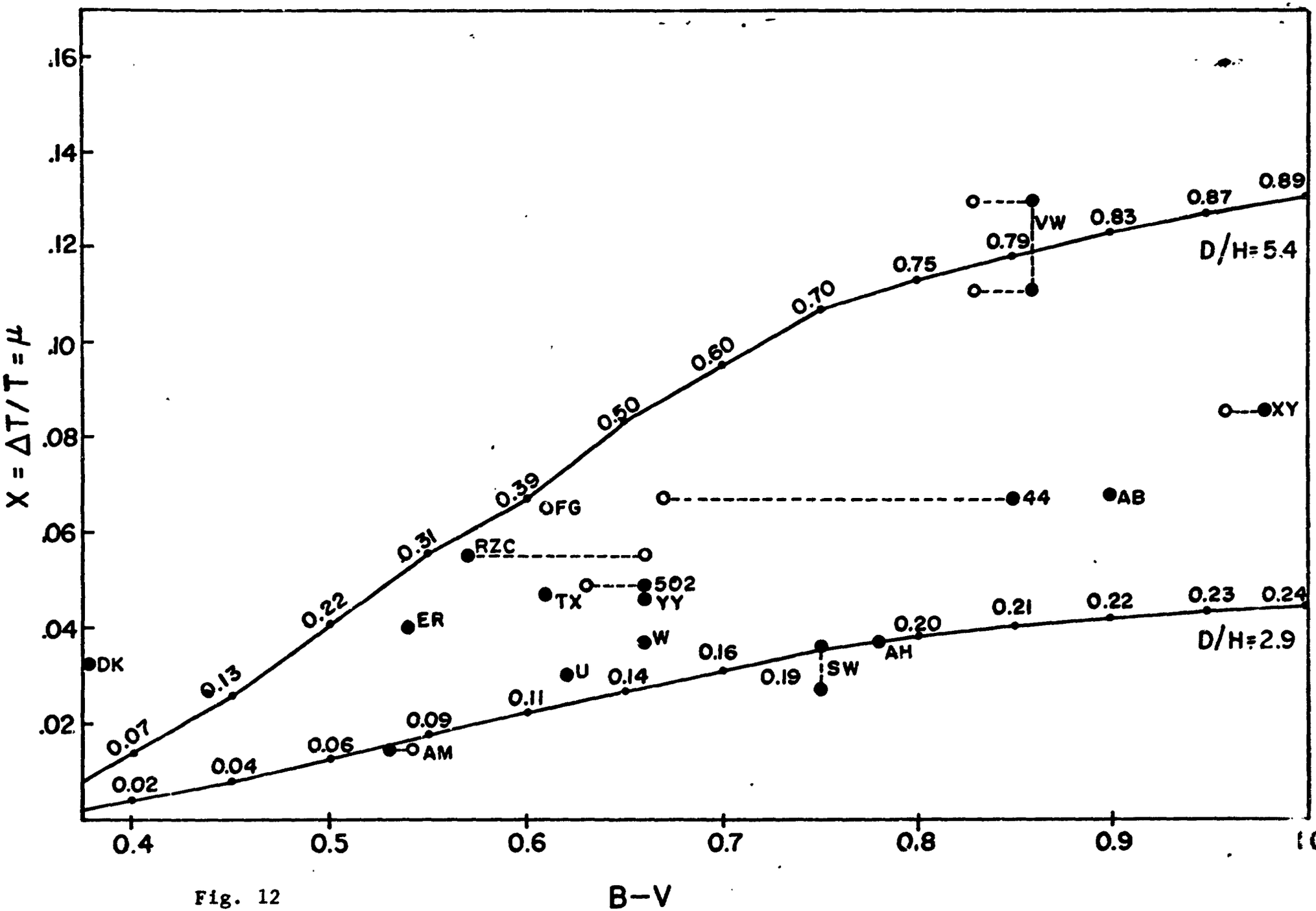
.16
.14
.12
.10
.08
.06
.04
.02
X = ΔT/T = μ
0.4
0.5
0.6
0.7
0.8
0.9
1.0
B−V
D/H=5.4
D/H=2.9
0.89
0.87
0.83
0.79
0.75
0.70
0.60
0.50
0.39
0.31
0.22
0.13
0.07
0.24
0.23
0.22
0.21
0.20
0.19
0.16
0.14
0.11
0.09
0.06
0.04
0.02
VW
XY
44
AB
OFG
RZC
502
YY
TX
ER
W
U
SW
AH
AM
DK

Fig. 12